39th Annual Condensed Matter and Materials Meeting

wagga2015

Charles Sturt University, Wagga Wagga, NSW
3 February 2015 – 6 February 2015

Australian and New Zealand Institutes of Physics

39th Annual Condensed Matter and Materials Meeting

Charles Sturt University, Wagga Wagga, NSW

3 February 2015 – 6 February 2015

CONFERENCE HANDBOOK

ISBN: 978-0-646-59459-0

WW2015 Organising Committee

Roger Lewis • Chao Zhang
Joseph Horvat • Enbang Li

Evan Constable • Julian Steele • John Mabon
Andrew Squires • Colin Bleasdale • Jarrod Colla

University of Wollongong, Wollongong, NSW 2522, Australia

wagga2015.com, wagga2015.info, wagga2015.net, wagga2015.org

@wagga2015, #wagga2015

WW 2015 SPONSORS

ammrf
Australian
Microscopy & Microanalysis
Research Facility

Australian Government

ansto

CSIRO

DOMO TECHNICA

ezzi vision
Vacuum and Thin Film Technology
www.ezzivision.com.au Freecall: 1800 GO EZZI

NSW GOVERNMENT Trade & Investment

Nucletron

scitek
total vacuum solutions

Stanton Scientific

WWZ

2015 CONTENTS

WW 2015 MAPS

Wagga Wagga and the location of the Charles Sturt University campus

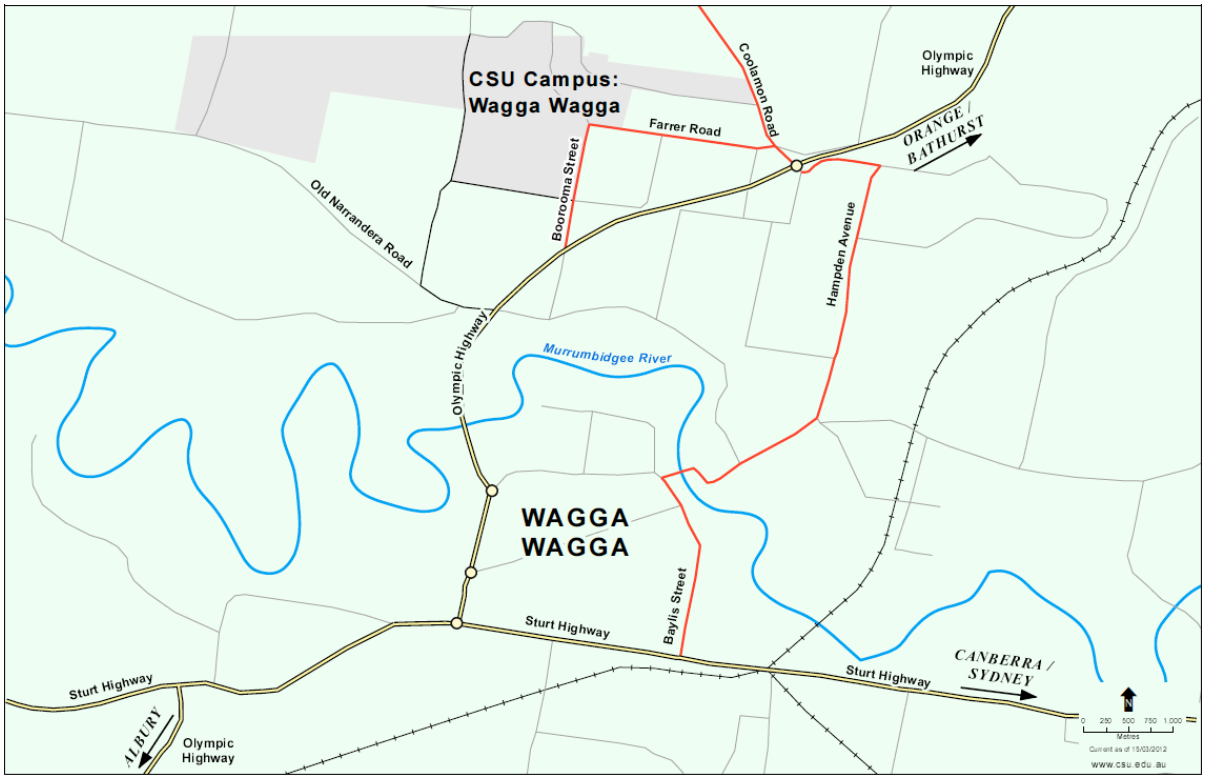

Charles Sturt University Convention Centre and Accommodation

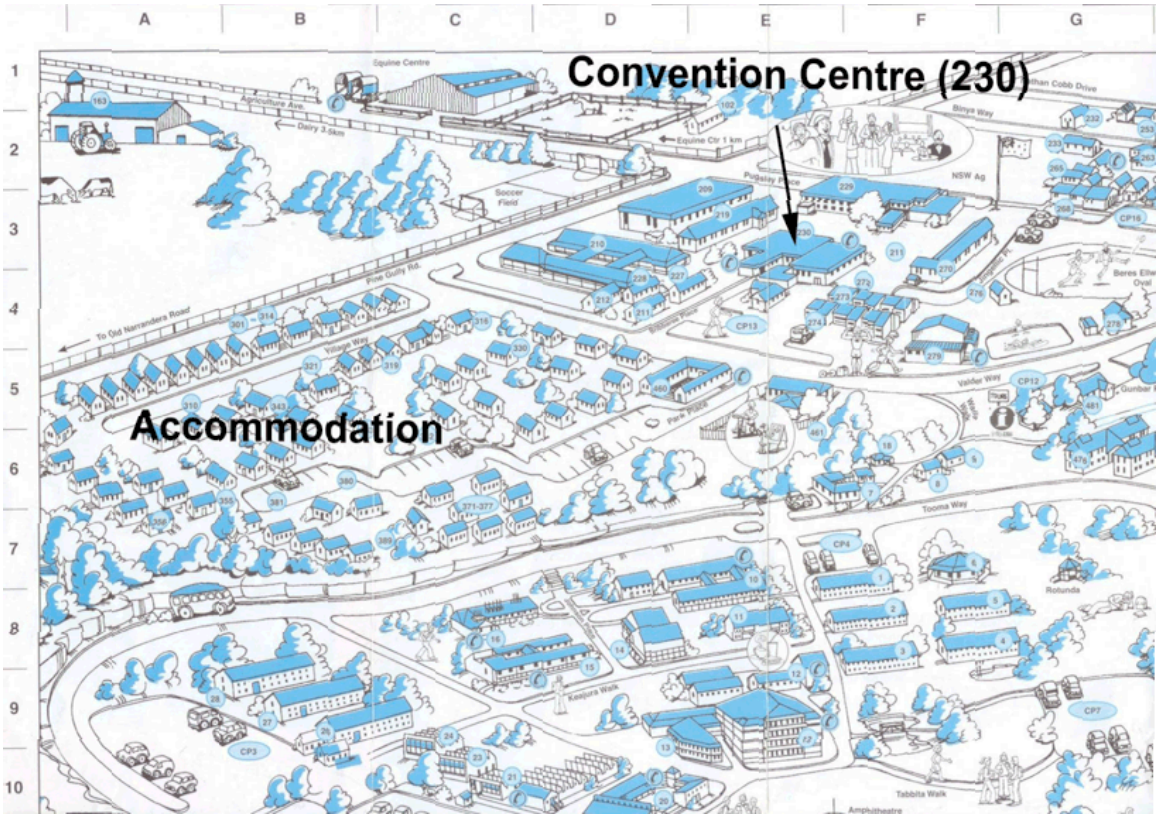

Charles Sturt University Convention Centre Map

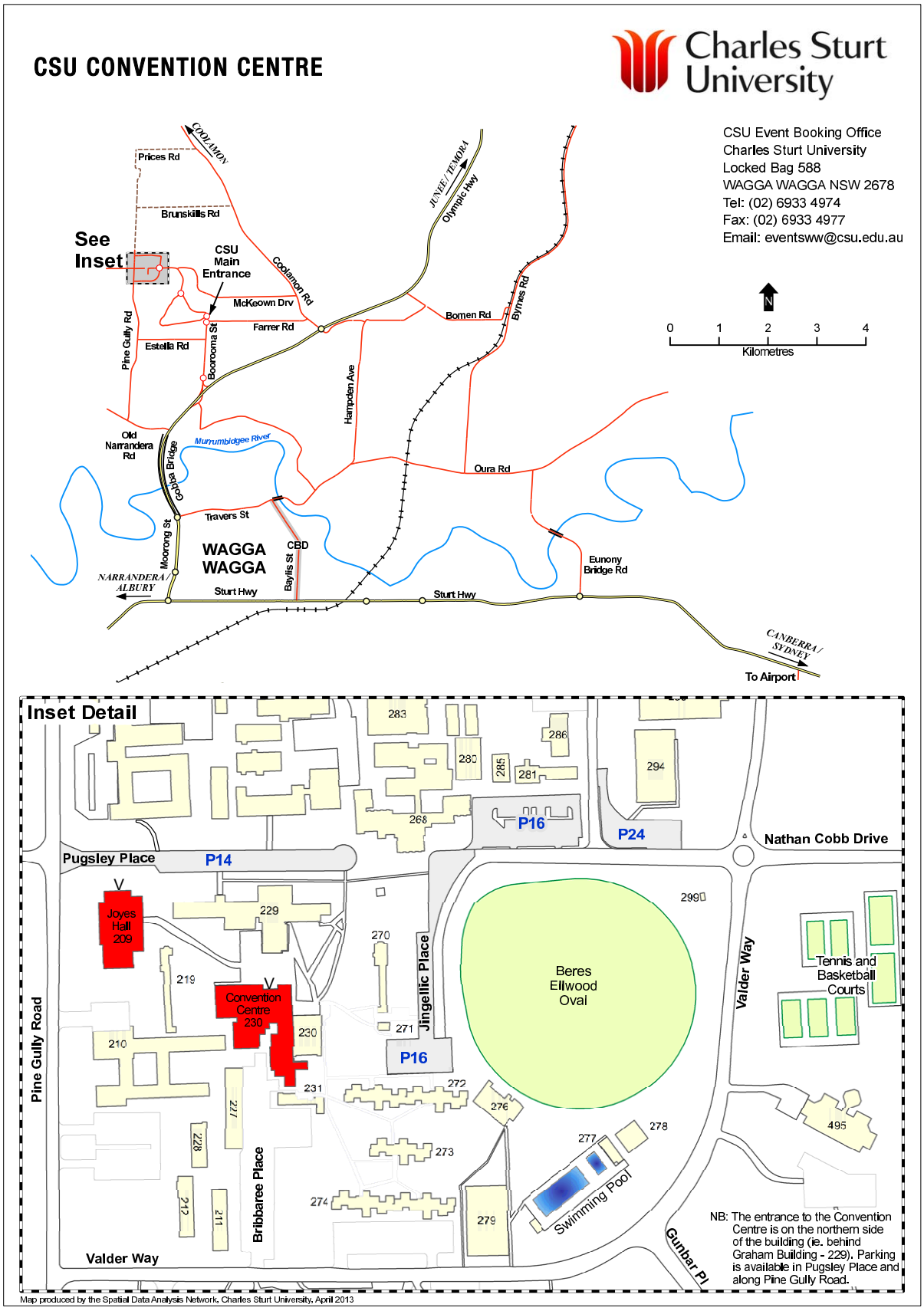

Wagga Wagga Campus Directory

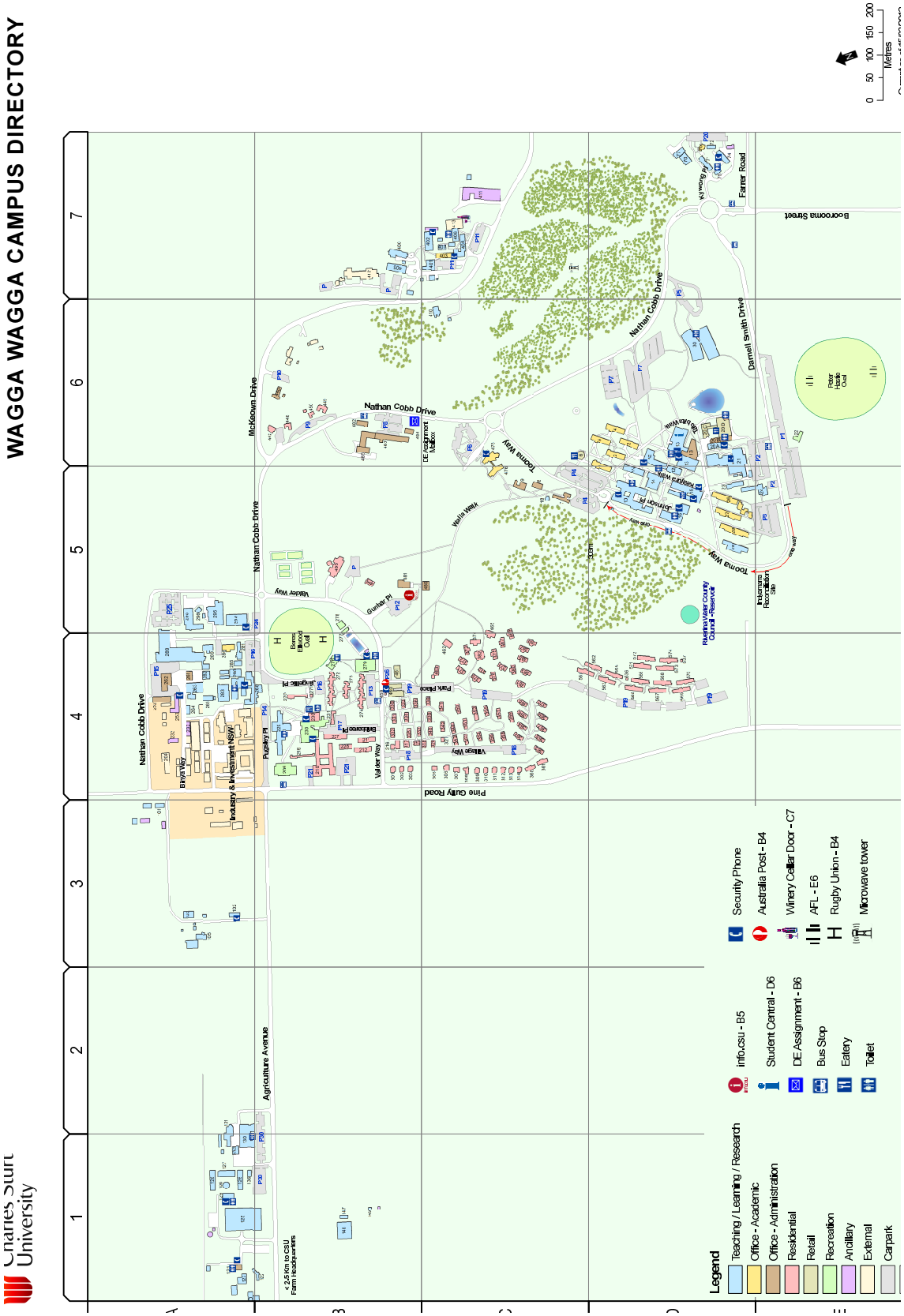

City of Wagga Wagga

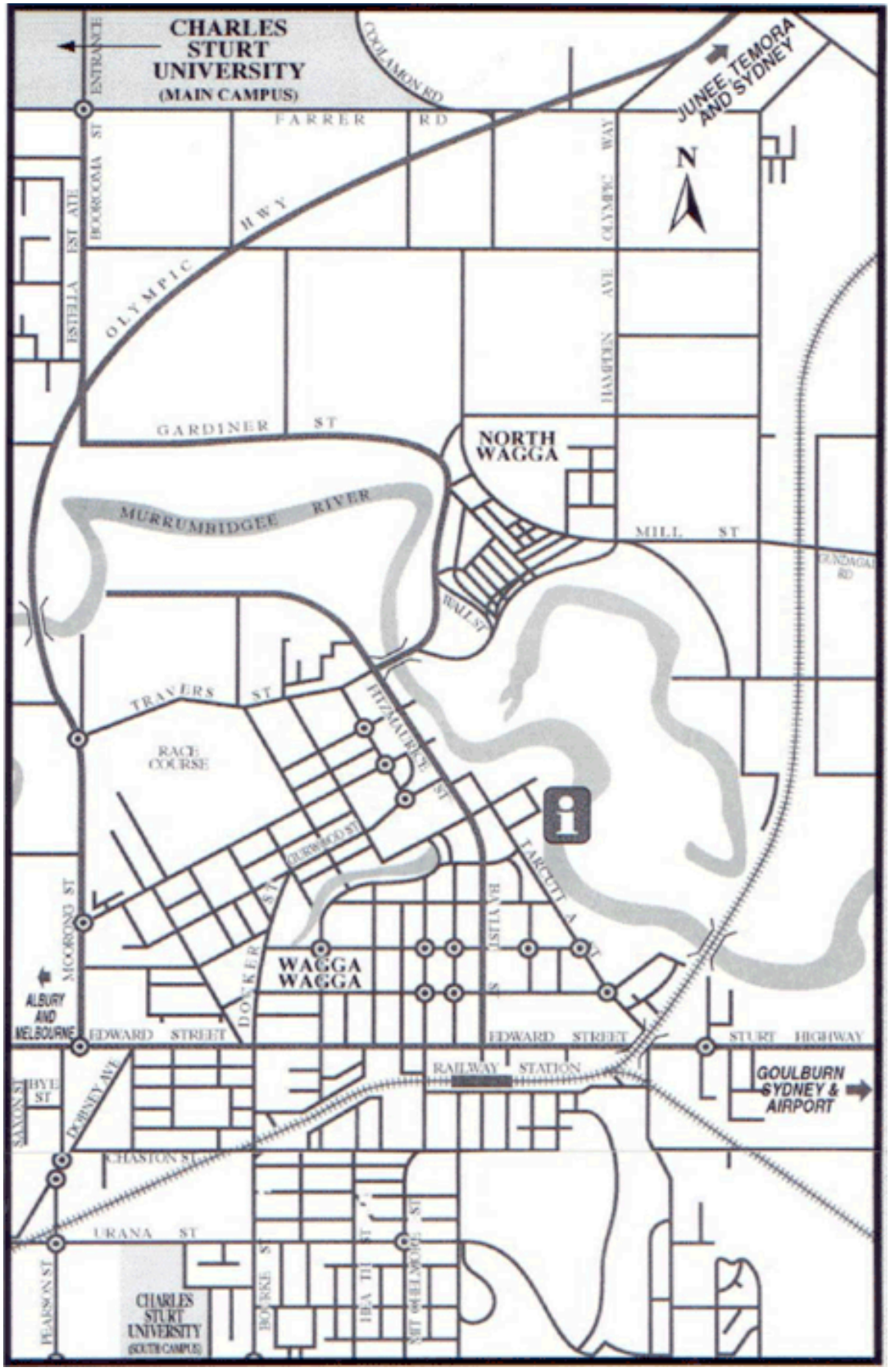

WW 2015 THE CMM GROUP

Welcome to the "Wagga" community

Just by attending the Annual Condensed Matter and Materials (CMM) Meeting you are a member of the CMM topical group of the Australian Institute of Physics (AIP). There are no forms or membership fees involved.

Take a look at the CMM Group web site

It can be accessed from the AIP national web site (*www.aip.org.au*) by clicking on **AIP Groups** listed under "Related Groups" in the column at the left of the home page and then selecting **Condensed Matter and Materials Group (CMM)**. Alternatively, you can go directly to *pems.unsw.adfa.edu.au/cmm*.

Please share your favourite "Wagga" experiences

If you have some special group images of you and colleagues, interesting events and stories from previous "Waggas", please share them with us by passing them on to Glen Stewart (*g.stewart@adfa.edu.au*) who will have them incorporated into the history section of the CMM Group web site. Please include in your e-mail the year of the meeting and the names of those "Waggarites" you are able to identify in the images.

1978

2002

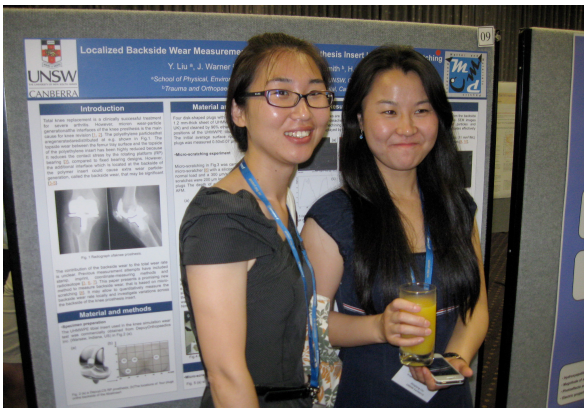

2012

2014

Perhaps you go all the way back to the good old days of sweltering lecture theatres without air conditioning, when the blokes loved their beards, floral body shirts, and Bermuda socks. There must be some great yarns and photographs lying around in the backs of minds and desk drawers, respectively.

2015 INFORMATION FOR PARTICIPANTS

Scientific Program:

All poster sessions and lectures will be held at the Convention Centre. Chairpersons and speakers are asked to adhere closely to the schedule for the oral program. A PC laptop computer and data projector, overhead projector, pointer and microphone will be available. Please check that your presentation is compatible with the facilities provided as early as possible. Posters should be mounted as early as possible. Please remove your Wednesday session posters by early Thursday morning and your Thursday session posters by the close of the program on Friday.

Logistics:

Please wear your name tag at all times. Registration and all other administrative matters should be addressed to the registration desk or a committee member. For lost keys or if locked out of your room from 0900 to 1700, contact Shiralee Hillam at the Events Office for assistance 6933 4974; after hours, contact the Accommodation and Security Office near the corner of Valder Way and Park Way or phone them at 6933 2288. Delegates must check out of their rooms on Friday morning, before 10:00.

Meals, Refreshments and Recreational Facilities:

All meals will be served in the dining room, except the Conference Dinner on Wednesday 6 February, which will be held in the Convention Centre. You will receive a dining room pass on registration and a ticket to the Conference Dinner. The dining room pass must be produced at every meal. It may also be required as identification for use of all other campus facilities, which are at your disposal.

Morning and afternoon tea will be served each day, as indicated in the timetable. Coffee and tea-making facilities are also available in the Common Room of each residence. In addition, on arrival on Tuesday afternoon and for the poster sessions, drinks will be available from the Conference Bar.

The swimming pool is open on weekdays from 12:00 until 18:00, as are the adjacent gymnasium (06:00-21:00) and squash courts. Tennis courts opposite the oval are also available. A wide range of facilities such as exercise bikes, weight training, table tennis, and basketball are available in the gymnasium. Access to these facilities is covered by your registration fee.

Convention Centre Contact Numbers:

Registration Desk Phone (02) 6933 4989
Convention Centre Office Phone (02) 6933 2606 Fax (02) 6933 2643
Events Office Phone (02) 6933 4974
After-hours Emergencies, Accommodation and Security Office Phone (02) 6933 2288
Internet access: wireless internet access is available within the Convention Centre (see *http://www.csu.edu.au/division/dit/wireless/index.htm*)

2015 SPONSOR DETAILS

Nucletron Pty Ltd
1b Little Commodore Street
Newtown, NSW 2042

Peter Douglas | Managing Director
e-mail: peter.douglas@au.nucletron.com
tel: +61 2 9517 1300
fax: +61 2 9517 1311
www.elekta.com/brachytherapy

Domo-Technica
PO Box 7077
Silverwater, NSW 2128

Michael Anderson
e-mail: Michael@domotech.com.au
tel: +61 2 9748 6955
fax: +61 2 9748 7855

www.domotech.com.au

WW77 Commemorative Shirt

Inaugurated in 2012 By Stewart Campbell, UNSW Canberra

Wagga 2012
- Green and Gold
- Male: L, XL
- Only six left!

Wagga 2013
- Black and White
- Male: S, M. L, XL, XXL
- Female: 8, 10, 12, 14

Wagga Wagga 1977
- Inaugural Meeting

Emblem

WW77 with Arrows
- Search all Directions
- Echo of AIP Logo

WW77 Commemorative Shirt
- Available for Purchase
  - Registration Desk
  - Limited Numbers
- Wagga2012
  - Green and Gold
- Wagga2013
  - Black and White

2015 PARTICIPANTS (at 23 January 2015)

	Participant		Affiliation	E-mail
1	Morgan	**Allison**	The University of Auckland	mall632@aucklanduni.ac.nz
2	Yee Sin	**Ang**	University of Wollongong	angy@uow.edu.au
3	Samuel	**Bladwell**	UNSW	leumas.llewdalb@gmail.com
4	Colin	**Bleasdale**	University of Wollongong	cb123@uowmail.edu.au
5	Alexys	**Bruno-Alfonso**	São Paulo State University (Unesp), Brazil	alexys@fc.unesp.br
6	Sean	**Cadogan**	ADFA	s.cadogan@adfa.edu.au
7	John	**Cashion**	Monash University	john.cashion@monash.edu.au
8	Fenfen	**Chang**	UNSW	fenfen.chang@unsw.edu.au
9	Hubert	**Chevreau**	ANSTO	hubertc@ansto.gov.au
10	Jarrod	**Colla**	University of Wollongong	jac050@uowmail.edu.au
11	Stephen	**Collocott**	CSIRO	stephen.collocott@gmail.com
12	Geoff	**Cousland**	University of Sydney	g.cousland@physics.usyd.edu.au
13	Yi	**Du**	University of Wollongong	ydu@uow.edu.au
14	Nancy	**Elewa**	UNSW	nancy.elewa@student.adfa.edu.au
15	Ivana	**Evans**	Durham University & ANSTO	ivana.radosavljevic@durham.ac.uk
16	Jacob	**Evans**	Macquarie University	jacob.evans@students.mq.edu.au
17	John	**Evans**	Durham University & ANSTO	john.evans@durham.ac.uk
18	Trevor	**Finlayson**	University of Melbourne	trevorf@unimelb.edu.au
19	Paul	**Graham**	UNSW	p.j.graham@unsw.edu.au
20	Joseph	**Horvat**	University of Wollongong	jhorvat@uow.edu.au
21	Wayne	**Hutchison**	UNSW Canberra	w.hutchison@adfa.edu.au
22	Gail	**Iles**	ANSTO	gail.iles@ansto.gov.au
23	Chennupati	**Jagadish**	ANU	c.jagadish@ieee.org
24	Ian	**Jackson**	ANU	ian.jackson@anu.edu.au
25	Scott	**Kang**	The University of Auckland	hkan026@aucklanduni.ac.nz
26	Yaroslav	**Kharkov**	UNSW	sushkov@phys.unsw.edu.au
27	Wataru	**Koshibae**	RIKEN	sushkov@phys.unsw.edu.au
28	Mikhail	**Kostylev**	UWA	mikhail.kostylev@uwa.edu.au
29	Wai Tung	**Lee**	ANSTO	wtl@ansto.gov.au
30	Roger	**Lewis**	University of Wollongong	roger@uow.edu.au
31	Enbang	**Li**	University of Wollongong	enbang@uow.edu.au
32	Tommy	**Li**	UNSW	tommyli@student.unsw.edu.au
33	Chris	**Ling**	University of Sydney	chris.ling@sydney.edu.au
34	Feng	**Liu**	University of Utah	fliu@eng.utah.edu
35	Rujun	**Liu**	Xian University of Technology	liurujun@xaut.edu.cn
36	Chris	**Lueng**	UWA	luengchris@gmail.com
37	Zhongshui	**Ma**	Peking University	mazs@pku.edu.cn
38	John	**Mabon**	University of Wollongong	nhojmabon@gmail.com
39	Ivan	**Maksymov**	UWA	ivan.maksymov@uwa.edu.au
40	Frederick	**Marlton**	UNSW	f.marlton@unsw.edu.au

41	Jeffrey	**McCallum**	University of Melbourne	jeffreym@unimelb.edu.au
42	Garry	**McIntyre**	ANSTO	garry.mcintyre@ansto.gov.au
43	Dimitry	**Miserev**	UNSW	sushkov@phys.unsw.edu.au
44	Michiyasu	**Mori**	UNSW	mori.michiyasu@jaea.go.jp
45	Jaan	**Oitmaa**	UNSW	j.oitmaa@unsw.edu.au
46	Wendy E	**Purches**	UNSW	w.purches@unsw.edu.au
47	Qingyong	**Ren**	UNSW Canberra	qingyong.ren@student.adfa.edu.au
48	Sven	**Rogge**	UNSW	s.rogge@unsw.edu.au
49	Kirrily	**Rule**	ANSTO	kirrily@ansto.gov.au
50	Matthew	**Sanderson**	University of Wollongong	ms919@uowmail.edu.au
51	Harley	**Scammell**	UNSW	sushkov@phys.unsw.edu.au
52	Jan	**Seidel**	UNSW	jan.seidel@unsw.edu.au
53	Jeff	**Sellar**	Monash University	jeff.sellar@monash.edu
55	Richard	**Skelton**	ANU	richard.skelton@anu.edu.au
55	Tilo	**Söhnel**	The University of Auckland	t.soehnel@auckland.ac.nz
56	Andrew	**Squires**	University of Wollongong	ads786@uowmail.edu.au
57	Julian	**Steele**	University of Wollongong	js598@uowmail.edu.au
58	Takanori	**Sugimoto**	Tokyo University of Science	sugimoto.takanori@rs.tus.ac.jp
59	Oleg	**Sushkov**	UNSW	sushkov@phys.unsw.edu.au
60	Manu	**Sushruth**	UWA	manu.sushruth@research.uwa.edu.au
61	Resta	**Susilo**	ADFA	resta.susilo@student.adfa.edu.au
62	Matthew	**Tate**	Durham University & ANSTO	matthew.tate@durham.ac.uk
63	Ivan	**Terekhov**	UNSW	sushkov@phys.unsw.edu.au
64	Giuseppe C	**Tettamanzi**	UNSW	g.tettamanzi@unsw.edu.au
65	Takami	**Tohyama**	UNSW	tohyama@rs.tus.ac.jp
66	Gordon	**Troup**	Monash University	gordon.troup@monash.edu.au
67	Clemens	**Ulrich**	UNSW	c.ulrich@unsw.edu.au
68	Tom	**Vogt**	U South Carolina & ANSTO	tvogt@mailbox.sc.edu
69	Zidong	**Wang**	The University of Auckland	zidong.wang@auckland.ac.nz
70	Christian	**Weickmann**	TU Darmstadt, Imp	weickmann@imp.tu-darmstadt.de
71	Leigh	**Weston**	University of Sydney	weston@physics.usyd.edu.au
72	Reyner	**White**	UNSW Canberra	reyner.white@student.adfa.edu.au
73	Julia	**Wind**	University of Sydney	jwin1641@uni.sydney.edu.au
74	Guangyong	**Xie**	Xian University of Technology	xiegy@xaut.edu.cn
75	Chunming	**Yin**	UNSW	c.yin@unsw.edu.au
76	Chao	**Zhang**	University of Wollongong	czhang@uow.edu.au
77	Jincheng	**Zhuang**	University of Wollongong	jz673@uowmail.edu.au

WW2015 PROGRAM OVERVIEW

Tuesday 3 February

16:00 –	Registration desk open
16:00 – 18:00	*Conference bar open*
18:00 – 19:30	*Dinner*
19:00 –	Posters WP1–WP16 to be mounted

Wednesday 4 February

07:30 – 08:30	*Breakfast*
08:45 – 09:00	Conference Opening
09:00 – 10:30	Oral Session: WM
10:30 – 11:00	*Morning tea*
11:00 – 12:45	Oral Session: WN
12:45 – 14:00	*Lunch*
14:00 – 15:30	Oral Session: WA
15:30 – 16:00	Poster Clips: WP1-WP16
16:00 – 16:30	*Afternoon Tea*
16:00 – 18:00	Poster Session: Papers WP1–WP16
18:00 –	Posters**:** TP1–TP16 to be mounted
18:30 – 22:00	*Conference Dinner*

Thursday 5 February

07:30 – 08:30	*Breakfast*
08:45 – 10:30	Oral Session: TM
10:30 – 11:00	*Morning tea*
11:00 – 12:30	Oral Session: TN
12:30 – 14:00	*Lunch*
14:00 – 15:30	Oral Session: TA
15:30 – 16:00	Poster Clips: TP1–TP16
16:00 – 16:30	*Afternoon Tea*
16:00 – 18:00	Poster Session: TP1–TP16
16:30 – 18:00	*Conference bar open*
18:00 – 19:30	*Dinner*
19:30 – 22:00	Trivia Quiz (Lindsay Davis Cup)

Friday 6 February

07:30 – 08:30	*Breakfast*
08:45 – 10:30	Oral Session: FM
10:30 – 11:00	*Morning tea*
11:00 – 12:30	Oral Session: FN
12:30 – 12:45	Presentations and Closing
12:45 – 14:00	*Lunch*

2015 PROGRAM DETAILS

Tuesday 3 February

16:00 –	Registration desk open
16:00 – 18:00	Conference bar open
18:00 – 19:30	Dinner

Wednesday 4 February

08:45 – 09:00		**Opening: *Roger Lewis, University of Wollongong***
09:00 – 10:30	**WM**	**Chairperson: *Chao Zhang, University of Wollongong***
09:00 – 09:30	WM1	Prediction of novel topological quantum materials *Feng Liu, University of Utah, USA* *INVITED*
09:30 – 09:45	WM2	Origins of Transition Metal Ordering in Infinitively Adaptive $Ln_2O_2MSe_2$-type Layered Oxychalcogenides *John S. O. Evans, Durham University, UK*
09:45 – 10:00	WM3	Spin wave dynamics in a ferromagnetic layer with the interface Dzyaloshinskii-Moriya interaction *M. Kostylev, University of Western Australia, Perth*
10:00 – 10:30	WM4	Nonequilibrium Charge Dynamics in One-Dimensional Extended Hubbard Model *Takami Tohyama, Tokyo University of Science, Japan* *INVITED*
10:30 – 11:00		**Morning Tea**
11:00 – 12:45	**WN**	**Chairperson: *Kirrily Rule, ANSTO***
11:00 – 11:30	WN1	Quantum Devices in Si and SiC Formed Using Ion Implantation *J. C. McCallum, University of Melbourne* *INVITED*
11:30 – 11:45	WN2	Quantum interference and quantum correlations in single dopants and exchange-coupled dopants in silicon *S. Rogge, University of New South Wales, Kensington*
11:45 – 12:00	WN3	Holmium Nitride: A ferromagnetic semiconductor with spintronic applications *J. P. Evans, Macquarie University*
12:00 – 12.45	ERA	0204 Condensed Matter Physics ERA insights *Marcus Nicol, Australian Research Council*
12:45 – 14.00		**Lunch**
14:00 – 15:30	**WA**	**Chairperson: *Wayne Hutchinson, UNSW Canberra***
14:00 – 14:30	WA1	Oxide Ion Conductors for Energy Applications: Twists and Hops in the Solid State *Ivana R. Evans, Durham University, UK* *INVITED*
14:30 – 14:45	WA2	Towards Superconducting-semiconducting Nano-hybrid devices *W. E. Purches, University of New South Wales, Kensington*
14:45 – 15:00	WA3	Strong eddy–current shielding of ferromagnetic resonance response in sub–skin–depth–thick conducting magnetic multilayers *I. S. Maksymov, University of Western Australia*
15:00 – 15:30	WA4	The Zeeman Effect and Hyperfine Structure of a Single Erbium Ion in Silicon *Chunming Yin, University of New South Wales* *INVITED*
15:30 – 16:00		**2-minute Poster Presentation:** WP1 - WP16
16:00 – 16:30		**Afternoon Tea (during Poster Session)**

16:00 – 18:00 Poster Session: WP1 – WP16

WP1 Thermodynamic Properties of a Heisenberg Model for the 'Quantum Spin-ice' Pyrochlore $Yb_2Ti_2O_7$.
J. Oitmaa and R. R. P Singh

WP2 Complementary Raman and Mössbauer Archaeological Studies
J. D. Cashion and W. H. Jay

WP3 Avalanche Behaviour at First-Order Phase Transitions
T.R. Finlayson and J.C. Lashley

WP4 First-Order Magnetic Phase Transition in TmGa
J.M. Cadogan and M. Avdeev

WP5 Residual Microstructure Effects of Mobile Bismuth Surface Droplets Formed during Molecular-beam-epitaxy of GaAsBi
J. A. Steele, R. A. Lewis, M. Henini, O. M. Lemine, D. Fan, Yu. I. Mazur, V. G. Dorogan, P. C. Grant, S.-Q. Yu and G. J. Salamo

WP6 Spin Splitting of Heavy Holes in Magnetic Focusing Experiments
S. Bladwell and O. P. Sushkov

WP7 The Lifetime of Magnons in the Vicinity of Quantum and Thermal Phase Transitions
H. D. Scammell and O. P. Sushkov

WP8 The Frequency-dependent Seismic Properties of Cracked and Fluid-saturated Glass-bead Media
Y. Li, E. C. David, I. Jackson and D. R. Schmitt

WP9 Magnetic ordering in $Er_2Fe_2Si_2C$ and $Tm_2Fe_2Si_2C$
R. A. Susilo, J. M. Cadogan, W. D. Hutchison, M. Avdeev, D. H. Ryan, T. Namiki and S. J. Campbell

WP10 Non-ergodicity in Praseodymium Oxide
J. R. Sellar

WP11 Spin-spiral to Spin-stripe Phase Transition Driven by Fluctuations
A. I. Milstein and O. P. Sushkov

WP12 Magnetic Structure of $TbRu_2Al_{10}$
R. White, W. D. Hutchison and T. Mizushima

WP13 Spin-charge Separation in 2D: Magnetization Density Induced by Spin 1/2 Impurity in the Vicinity of Quantum Critical Point
Y. Kharkov, I. Terekhov and O. Sushkov

WP14 The Apparent Neglect of the Effects on 'Winehealth', and in Wines, of 'Radical Ions'
Gordon J. Troup, and Simon Drew

WP15 The Magnetic Ground State of Dy^{3+} in $DyNiAl_4$
W. D. Hutchison, G.A. Stewart and J. M. Cadogan

WP16 Synchrotron Powder Diffraction Investigations of the Crystal Structure of the Solid Solution $Cu_{1-x}Co_xSb_2O_6$
H.-B. Kang, T.R. Finlayson and T. Söhnel

18:30 – 22:00 **Conference Dinner**

After Dinner Talk
Science in Space: Reality vs. Fiction
Gail N. Iles, ANSTO *INVITED*

Thursday 5 February

08:45 – 10:30	**TM**	**Chairperson: *Clemens Ulrich, University of New South Wales***
08:45 – 09:15	TM1	Semi-classical orbits of phosphorus donors in silicon under a magnetic field *Alexys Bruno-Alfonso, São Paulo State University, Brazil* *INVITED*
09:15 – 09:30	TM2	Elasticity of lizardite-1T from dispersion-corrected DFT *R. Skelton, Australian National University*
09:30 – 09:45	TM3	Exploring the properties of mixed cobalt/iron/manganese-tin clusters *M. Allison, University of Auckland, New Zealand & University of Sydney*
09:45 – 10:00	TM4	Effects of 18O isotope substitution in multiferroic RMnO3 (R=Tb, Dy) *P. J. Graham, University of New South Wales*
10:00 – 10:15	TM5	Structural properties of the Nb-doped bismuth oxide materials, $Bi_{1-x}Nb_xO_{1.5+x}$ *M. L. Tate, ANSTO & University of Durham, UK*
10:15 – 10:30	TM6	The magneto-structural transition in magnetocaloric $Mn_{1-x}Fe_XCoGe$ *Q. Y. Ren, University of New South Wales, Canberra*
10:30 – 11:00		**Morning Tea**
11:00 – 12:30	**TN**	**Chairperson: *Mikhail Kostylev, University of Western Australia***
11:00 – 11:30	TN1	Dynamics of magnetic skyrmions: Theoretical design of skyrmion devices *W. Koshibae, RIKEN, Japan* *INVITED*
11:30 – 11:45	TN2	Pressure-induced inter-site valence transitions involving geometric frustration in hexagonal perovskites *Chris D. Ling, University of Sydney*
11:45 – 12:00	TN3	Violation of the Spin Statistics Theorem and the Bose-Einstein Condensation of Particles with Half Integer Spin *H. D. Scammell, University of New South Wales, Kensington*
12:00 – 12:15	TN4	Yttria-stabilised zirconia: A trend study of structural, electronic and vibrational properties *G. P. Cousland, University of Sydney & ANSTO*
12:15 – 12:30	TN5	*Electron-Phonon Coupling in Epitaxial Silicene: Scanning Tunneling Microscopy and Raman Studies* *Y. Du, University of Wollongong*
12:30 – 14.00		**Lunch**

14:00 – 15:30 TA Chris D. Ling, University of Sydney

14:00 – 14:30 TA1 Domain walls and phase boundaries - new nanoscale functional elements
Jan Seidel, University of New South Wales, Kensington *INVITED*

14:30 – 14:45 TA2 Cobalt-palladium multilayer films for hydrogen gas sensing
Chris Lueng, University of Western Australia

14:45 – 15.00 TA3 Polarised Neutrons for Materials Research on OPAL Instruments
W. T. Lee, ANSTO

15:00 – 15:15 TA4 ^{57}Fe Mössbauer Study of the Chainpur meteorite
Nancy N. Elewa, University of New South Wales, Canberra

15:15 – 15:30 TA5 Neutron scattering's influence on crystallography
G. J. McIntyre, ANSTO

15:30 – 16:00 2-minute Poster Presentation: TP1 – TP16

16:00 – 16:30 Afternoon Tea (during Poster Session)

16:00 – 18:00 Poster Session: TP1 – TP16

TP1 EMU, the Cold-Neutron Backscattering Spectrometer at the Bragg Institute, ANSTO
N. de Souza, A. Klapproth and G. N. Iles

TP2 Mössbauer observation of the Mobility of Cl- Ions in a Frozen Solution
J. D. Cashion, T. K. Choo and L. Zhang

TP3 Cusp Singularities and Magnetization Plateaux in a Frustrated Spin Ladder
T. Sugimoto, M. Mori, T. Tohyama, and S. Maekawa

TP4 The Square Lattice Quantum ANNNH Model Revisited: Does the Model Support a '2+2' Phase?
J. Oitmaa, and R. R. P Singh

TP5 Terahertz Emission by Ultrafast Cathode Erosion Processes in Electrical Discharge
J. Horvat, E. Constable and R. A. Lewis

TP6 Confinement due to spin-orbit interaction in quantum point contacts
T. Li

TP7 Strong Spin-orbit Coupling Effects Driven by an External Magnetic Field and the Anisotropic Zeeman Effect in 2D GaAs (InAs) Quantum Dots
D. S. Miserev and O. P. Sushkov

TP8 Electron Tunneling Across Potential Barrier in AA-stacked Graphene
M. Sanderson, Y. S. Ang and C. Zhang

TP9 Enhancement of Magnon Mediated Coupling between Fermions in a Vicinity of a Magnetic Quantum Critical Point
Y. Kharkov and O. Sushkov

TP10 The Capacitive Current and Conduction Current of Zinc Oxide Varistor Ceramic Materials for Nanosecond Pulse Electronic Breakdown
G. Xie and W. Shi

TP11 Effects of Coulomb Screening and Disorder on Artificial Graphene Based on Nanopatterned Semiconductor
O. A. Tkachenko, V. A. Tkachenko, I. S. Terekhov and O. P. Sushkov

TP12 Evolution of Magnetic Phase and Cation Distribution in $Cu_{1-x}Zn_xFe_2O_4$ Studied by Neutron Powder Diffraction
F. F. Chang, G. C. Deng, M. Avdeev, J. Bertinshaw, J. Hester and C. Ulrich

TP13 Enhancement of T_C in Fe-Based Superconducting Films by Strain Effect
J. C. Zhuang, Y. Du, X. Xu, and S. X. Dou

TP14 The Magnetic Properties and Magnetocaloric Effect in $Mn_{1-x}Ni_xCoGe$
Q. Y. Ren, W. D. Hutchison, J. L. Wang, A. J. Studer and S. J. Campbell

TP15 3D Printed Terahertz Diffraction Gratings and Lenses
A. D. Squires, E. Constable and R. A. Lewis

TP16 Combinatorial Synthesis of Piezoelectric Materials Using an Inkjet printer
F. Marlton, J. Daniels and O. Standard

18:00 – 19:30 **Dinner**

19:30 – 22:00 **Trivia Quiz (Lindsay Davis Cup)**

Friday 6 February

08:45 – 10:30	**FM**	**Chairperson: *Oleg Sushkov, UNSW Kensington***
08:45 – 09:15	FM1	Phonon Hall effect in the terbium-gallium-garnet: Skew scattering of phonon *Michiyasu Mori, Japan Atomic Energy Agency, Japan* *INVITED*
09:15 – 09:30	FM2	Adsorption of CO_2 and CD_4 in UiO-66: a combination of neutron diffraction and modelling *H. Chevreau, ANSTO*
09:30 – 09:45	FM3	Spin-lattice coupling and multiferroic effects for $3d^4$ – $3d^7$ dopants in a ferroelectric host materials *L. Weston, University of Sydney*
09:45 – 10:00	FM4	Strain-induced magnetic phase transition in $SrCoO_3$ thin films *C. Ulrich, University of new South Wales, Kensington*
10:00 – 10:15	FM5	Measuring Liquid Crystal Permittivity With High Accuracy *Christian Weickhmann, Technische Universität Darmstadt, Germany*
10:15 – 10:30	FM6	Spin dynamics simulation of the magneto-electric effect in a composite multiferroic chain *Zidong Wang, University of Auckland, New Zealand*
10:30 – 11:00		**Morning Tea**
11:00 – 12:30	**FN**	**Chairperson: *Garry McIntyre, ANSTO***
11:00 – 11:15	FN1	Commensurate to incommensurate magnetic phase transition in the type-II multiferroic $YBaCuFeO_5$ *Kirrily Rule, ANSTO*
11:15 – 11:30	FN2	Synthesis and characterisation of $(M_{2-x}Fe_x)SnO_4$ (M = Mn, Zn) quaternary transition metal-tin-oxygen spinel systems *T. Söhnel, University of Auckland, New Zealand*
11:30 – 11:45	FN3	A combined experimental and computational approach to understanding and developing solid-state ionic conductors *J. Wind, University of Sydney*
11:45 – 12:00	FN4	Magnonic crystals for nanoparticle detection *M. Sushruth, University of Western Australia*
12:00 – 12:30	FN5	Semiconductor Nanowires for Optoelectronics and Energy Applications *Chennupati Jagadish, Australian National University* *INVITED*
12:30 – 12:45		**Closing** *Roger Lewis, University of Wollongong*
12:45 – 14:00		**Lunch**

WEDNESDAY ABSTRACTS

WM1

Prediction of novel topological quantum materials

F. Liu

Department of Materials Science and Engineering, University of Utah, Salt Lake City, UT 84112, USA.

Topological insulators (TIs) are a recently discovered class of materials having insulating bulk electronic states but conducting boundary states distinguished by nontrivial topology. So far, several generations of TIs have been theoretically predicted and experimentally confirmed. In this talk, I will first present our recent theoretical prediction of a new family of 2D "organic" TIs made of organometallic lattices [1-4], based on first-principles calculations and tight-binding model analyses. Designed by assembling molecular building blocks of organometallic compounds with strong spin-orbit coupling into a hexagonal and Kagome lattices, these new classes of organic topological materials are shown to exhibit nontrivial topological edge states in both Dirac bands [1,4] and flat Chen bands (so-called fractional Chern insulator) [2,4], which are robust against significant lattice strain. Realisation of half metallic state and anomalous quantum Hall effect in magnetic organic TIs with the inclusion of transition metal elements will also be discussed [3]. Then, I will discuss our most recent studies of large-gap topological phases on conventional semiconductor surfaces [5,6]. By epitaxial growth of heavy metal elements such as Bi on a halogenated Si(111) surface, a large-gap (~0.8 eV) quantum spin Hall state [5] is shown to originate from an intriguing substrate orbital filtering effect that critically select the orbital composition around the Fermi level to form different topological phases. Furthermore, growth of transition metals such as W leads to formation of a new form of 2D material, so-called sd^2 graphene [6], which is characterised with bond-centered electronic hopping that transforms the apparent atomic hexagonal lattice into the physics of Kagome lattice to exhibit room-temperature quantum anomalous Hall state. We envision that these findings will greatly broaden the scientific scope and technological impact of emerging topological materials.

[1] Z.F. Wang, Z. Liu and F. Liu, *Nature Commun*. **4**, 1471 (2013).

[2] Z. Liu, Z. F. Wang, J.-W. Mei, Y. Wu and F. Liu, *Phys. Rev. Lett.* **110**, 106804 (2013).

[3] Z.F. Wang, Z. Liu and F. Liu, *Phys. Rev. Lett.* **110**, 196801 (2013).

[4] Z.F. Wang, N. Su and F. Liu, *Nano Lett.* **13**, 2842 (2013).

[5] M. Zhou, *et al., Proc. Natl. Acad. Sci.* **111**, 14378 (2014).

[6] M. Zhou, Z. Liu, W. Ming, Z. Wang, and F. Liu, *Phys. Rev. Lett.* **113**, 236802 (2014).

WM2

Origins of Transition Metal Ordering in Infinitively Adaptive $Ln_2O_2MSe_2$-type Layered Oxychalcogenides

C.M. Ainsworth,[a] C.-H. Wang,[a] H.E. Johnston,[a] E.E. McCabe,[a] M.G. Tucker,[b] J.S.O. Evans[a]

[a] *Department of Chemistry, University Science Site, Durham University, South Road, Durham, UK, DH1 3LE.*

[b] *ISIS Neutron and Muon Source, Science and Technology Facilities Council, Rutherford Appleton Laboratory, Harwell, Oxford, Didcot, UK, OX11 0QX.*

Email: john.evans@durham.ac.uk, web site: https://community.dur.ac.uk/john.evans/index.html

A number of *Ln*OCu*Ch*-related compounds with composition $Ln_2O_2MSe_2$ (Ln = La & Ce, M = Fe, Zn, Mn & Cd) have been reported in the literature, built from alternating layers of fluorite-like $[Ln_2O_2]^{2+}$ sheets and antifluorite-like $[MSe_2]^{2-}$ sheets. They all contain divalent transition metal ions leading to half occupancy of tetrahedral sites in the selenide layers. The ordering of the transition metals is different across the known structures: $[MSe_2]^{2-}$ layers can either contain MSe_4 tetrahedra that are exclusively edge-sharing (E, stripe-like), exclusively corner-sharing (C, checkerboard-like), or sections of both. This work reveals the origins of this ordering by investigating a range of solid solutions. Substitution of *M* leads to changes almost entirely in the *c* parameter, perpendicular to the layers, whereas substitution of *Ln* leads to an approximately isotropic change in all lattice parameters. This is attributed to a relatively rigid *Ln*-O layer and a flexible *M*-Se layer, which adapts to the size demands of the *Ln*-O layer. Transition metal ordering is determined by the relative sizes of $[Ln_2O_2]^{2+}$ and $[MSe_2]^{2-}$ layers, and can be tuned by doping in either layer. A progressive evolving range of commensurate and incommensurate compounds will be reported showing that the materials can be considered as infinitively adaptive structures.

WM3

Spin wave dynamics in a ferromagnetic layer with the interface Dzyaloshinskii-Moriya interaction

M. Kostylev[a], A.A. Stashkevich[b], M. Belmeguenai[b] and Y. Roussigné[b]

[a] *School of Physics, University of Western Australia, Crawley 6009, WA, Australia.*

[b] *LSPM (CNRS-UPR 3407), Université Paris 13, 93430 Villetaneuse, France.*

The interfacial Dzyaloshinskii-Moriya interaction (IDMI) has been a subject of significant interest recently [1-4]. In the present work we study theoretically and experimentally the dispersion of the Damon-Eshbach spin waves (DESW) in ferromagnetic films with IDMI and spatially uniform ground state of magnetisation. Theoretically we show that the effect of IDMI on DE MSSW may be described as a new type of exchange boundary conditions (EBC) for the vector of dynamic magnetisation at a ferromagnetic layer surface (interface) where IDMI is present. The derived EBC demonstrate that IDMI leads to pinning of dynamic magnetisation at the interface. An unusual peculiarity of the IDMI-based pinning is that it scales as the spin-wave wave number k and is of opposite signs for the clockwise and counter-clockwise rotating components of the dynamic magnetisation vector.

Experimentally we measure DESW dispersion in Pt/$Ni_{80}Fe_{20}$ bilayer films using Brillouin light scattering technique (BLS). The interface between the non-magnetic Pt and ferromagnetic NiFe introduces IDMI in NiFe. We observe a significant frequency shift of spin waves due to IDMI. The shift scale linearly with k and is of opposite signs for the waves propagating in the two opposite directions in the film plane. The frequency shift is large and easily measurable with BLS. In particular, for Pt[6nm]/NiFe[4nm] sample the shift reaches 200 MHz for k=20 μm^{-1}. This result is in good agreement with the constructed theory.

Financial support by the Australia Research Council and the University of Western Australia is acknowledged.

[1] G. Chen, et al., *Phys.Rev.Lett.* **110**, 177204 (2013).

[2] S. Emori, et al., *Nat.Mater*. **12**, 611 (2013).

[3] Jung-Hwan Moon, et al., *Phys. Rev. B* **88**, 184404 (2013).

[4] M. Kostylev*, J. Appl. Phys*. **115**, 233902 (2014).

WM4

Nonequilibrium Charge Dynamics in One-Dimensional Extended Hubbard Model

T. Tohyama

Department of Applied Physics, Tokyo University of Science, Tokyo 125-8585, Japan.

One-dimensional extended Hubbard model at half filling shows a spin-density-wave (SDW) state and charge-density-wave (CDW) state depending on the relative strength of on-site Coulomb interaction (U) and inter-site Coulomb interaction V. We investigate the photo-induced charge dynamics and nonequilibrium process of the model driven by transient laser pulse by using the time-dependent Lanczos method. In the case of large U and U~2V, the SDW and CDW phases are separated by a first order phase transition. When the system is subjected to the irradiation of a laser pulse in the SDW phase near the phase boundary, we find that a sustainable charge order enhancement can be realised with proper laser frequency and strength, while local spin correlations remains [1]. We analyze the conditions and investigate possible mechanisms of the emerging order enhancements. Secondly, we investigate the ultrafast optical response of the model exposed to two successive laser pulses [2]. We find that following the first pulse, the excitation and deexcitation process between the ground state and excitonic states can be precisely controlled by the relative temporal displacement of the pulses. The underlying physics can be understood in terms of a modified Rabi model. Thirdly, we examine the time-dependent optical conductivity [3]. In the SDW phase, the optical conductivity shows a clear low-energy excitation after pumping. On the other hand, a mid-gap state appears in the optical conductivity when CDW states are pumped. The implications of these results will be discussed.

[1] H. Lu, S. Sota, H. Matsueda, J. Bonca and T. Tohyama, *Phys. Rev. Lett.* **109**, 197401 (2012).

[2] H. Lu, J. Bonca and T. Tohyama, *EPL* **103**, 57005 (2013).

[3] H. Lu, D. Manske, J. Bonca and T. Tohyama, in preparation.

WN1

Quantum Devices in Si and SiC Formed Using Ion Implantation

J.C. McCallum[a], M. Stuiber[a], A. Lohrman[a], N. Iwamoto[b], T. Ohshima[b] and B.C. Johnson[a]

[a] *Centre of Excellence for Quantum Computation and Communication, School of Physics, University of Melbourne, Victoria 3010, Australia.*

[b] *Semiconductor Analysis and Radiation Effects Group, Japan Atomic Energy Agency, 1233 Watanuki, Takasaki, Gunma 370-1292, Japan.*

Single ion implantation and ion implantation at low fluences are being used to fabricate quantum devices in the Centre for Quantum Computation and Communication Technology (CQC2T) in Australia [1]. In silicon, recent breakthroughs include coherent manipulation of an individual electron spin qubit bound to a phosphorus donor atom in natural Si with single-shot read-out [2], single shot read-out of the nuclear spin of a single ^{31}P atom with very high readout fidelity and operation of the single nuclear spin as a qubit [3], a coherence time T_2 exceeding 30 s for a single electron spin in isotopically pure ^{28}Si epilayers [4] and observation of the optical excitation of a single erbium atom implanted in the channel of a silicon transistor [5]. In all of these devices the quantum bits (qubits) have been created using ion implantation. Ion implantation can also be used to form defect centres in diamond and SiC that act as single photon sources with applications in quantum computation and communications. In this presentation I will discuss the range of devices we have produced and the ion implantation strategies used in their fabrication, including single ion implantation methodologies and use of molecular implant species. I will also briefly describe some of the challenges and future directions of our research.

[1] J.C. McCallum, et al., *Adv. Mater. Sci. Eng*. **2012**, 272694, (2011).

[2] J.J Pla, et al., *Nature* **488**, 541, (2013).

[3] J.J. Pla, et al., *Nature* **496**, 334, (2013).

[4] J.T. Muhonen, et al., *Nature Nanotechnol.* **9**, 986–991 (2014)

[5] C. Yin, et al., *Nature* **497**, 91, (2013).

WN2

Quantum interference and quantum correlations in single dopants and exchange-coupled dopants in silicon

J. Salfi[a], J. A. Mol[a], R. Rahman[b], G. Klimeck[b], M. Y. Simmons[a], L. C. L. Hollenberg[c] and S. Rogge[a]

[a] *Centre for Quantum Computation and Communication Technology, School of Physics, The University of New South Wales, Sydney, New South Wales 2052, Australia.*

[b] *Purdue University, West Lafayette, Indiana 47906, USA.*

[c] *Centre for Quantum Computation and Communication Technology, School of Physics, University of Melbourne, Parkville, Victoria 3010, Australia.*

Quantum electronics exploiting the highly coherent states of single dopants in silicon invariably requires interactions between states and interfaces, and inter-dopant coupling by exchange interactions. We have developed a low temperature STM scheme for spatially resolved single-electron transport in a device-like environment, providing the first wave-function measurements of single donors and exchange-coupled acceptors in silicon. For single donors, we directly observed valley quantum interference due to linear superpositions of the valleys [1], and found that valley degrees of freedom are highly robust to the symmetry-breaking perturbation of nearby (3 nm) surfaces. For exchange-coupled acceptors, we measured the singlet-triplet splitting, and from the spatial tunneling probability, extracted information about the 2-body wavefunction amplitudes and determined the entanglement entropy[2], a measure of the inseparability (quantum correlations) generated by the interactions between their indistinguishable particles. Entanglement entropy of the J=3/2 holes was found to increase with increasing dopant distance, as Coulomb interactions overcome tunneling, coherently localizing spin towards a Heitler-London singlet, mimicking S=1/2 particles [3]. In the future these capabilities will be exploited to peer into the inner workings of few-dopant devices and shed new light on multi-dopant correlated states, engineered atom-by-atom.

[1] J. Salfi *et al*., *Nature Mat.* **13** 605 (2014).

[2] L. Amico *et al.*, *Rev. Mod. Phys.* **80** 517-576 (2008).

[3] J. Salfi *et al.*, (2014) submitted.

WN3

Holmium Nitride: A ferromagnetic semiconductor with spintronic applications

J.P. Evans and J.E. Downes

MQ Photonics Research Centre, Department of Physics and Astronomy – Macquarie University, NSW 2109, Australia.

Rare-Earth Nitrides (REN's) are quite unique in intrinsically possessing ferromagnetic and semiconducting properties simultaneously. Ferromagnetic semiconductors possess properties ideal for spintronics, where the charge and spin of the electron is used to process information. One such REN is Holmium Nitride (HoN).

HoN is a promising intrinsic ferromagnetic semiconductor. Using nanocrystalline thin films grown by Ion Assisted Deposition, we have observed a direct bandgap of approximately 2.03 eV, and a Curie temperature of approximately 18 K. We have also found unusual results of rare-earth 4*f* electron hybridisation [1] and a lower than expected magnetic moment per ion [2].

We have found the growth conditions play a significant role in determining the crystal structure. I will report how the substrate temperature, growth rate, nitrogen pressure, and the nitrogen state can be optimised to improve crystal quality. I will also discuss different substrates and how they affect the crystal structure, as well as other techniques to improve the crystal quality.

I will also report the first ever growth of mixed REN thin films. Specific attention will be on $Dy_xHo_{x-1}N$. The magnetism of these materials, and their crystal structure will be reported for ratios of x = 0.05, 0.25, 0.5, 0.75, and 0.95.

[1] J.D. Brown *et al. Appl. Phys. Lett*. **100**, 072108 (2012).

[2] D.L. Cortie *et. al.*, *Phys. Rev. B* **89**, 064424 (2014).

WA1

Oxide Ion Conductors for Energy Applications: Twists and Hops in the Solid State

I.R. Evans,[a] X. Kuang,[a] J.L. Payne, [a] J.D. Farrell[a] and M.R. Johnson[b]

[a] *Department of Chemistry, Durham University, Durham DH1 3LE, U.K.*

[b] *Institut Laue Langevin, Grenoble, F-38042, France.*

Meeting the future energy needs of the world's growing population is one of today's most significant scientific challenges. Different types of new, renewable and sustainable energy generation have been the subject of intense research, including solar, nuclear, wind and geothermal energy. Solid oxide fuel cell (SOFC) technology is a frontrunner in the short-to-medium term race to provide sustainable energy solutions, owing to the unique combination of high efficiency, fuel flexibility and environmental safety. Two factors have prevented the widespread commercialisation of SOFCs: system cost and reliability, and both stem from the high operating temperatures of the current technology (850–1000^{o}C). Lowering the operating temperatures into the so-called intermediate temperature region (500–700^{o}C) is therefore a major driver in SOFC research.

We have recently reported exceptional low-temperature oxide ion conductivity in $Bi_{1-x}V_xO_{1.5+x}$ (x = 0.095–0.087) phases, with $\sigma = 3.5\times10^{-2}$ S/cm at 450^{o}C, the highest to-date in a stable 3D fluorite-type system. We have attributed this remarkable behaviour to the simultaneous presence of four key structural factors: a highly polarisable sublattice with vacancies, central atoms able to support variable coordination numbers and geometries, and the rotational flexibility of these coordination polyhedra, co-existing in a pseudo-cubic structure. We have found similar structural features to lead to high oxide ion conductivity in a number of other materials with complex superstructures (vanadates, molybdates, tungstates, rhenates).

This presentation will focus on the new materials discovered and characterised and the crystallographic methods used to characterise them. In particular, it will illustrate how a combination of careful crystallographic work, computational methods and characterisation of physical properties is required to understand the complexity of next- generation functional materials.

Towards superconducting-semiconducting nano-hybrid devices

W.E. Purches[a,c], A. Rossi[b,], A. S. Dzurak[b,c], S. Rogge[a,c] and G.C. Tettamanzi[a,c]

[a] *School of Physics, UNSW, Australia.*

[b] *School of Electrical Engineering and Telecommunications, UNSW, Australia.*

[c] *Centre for Quantum Computation and Communication Technology, UNSW, Australia.*

The Josephson Field Effect Transistor (JOFET) combines the speed and low power consumption of superconductors with the tunability of field effect devices [1]. Nano-scale JOFETs hold considerable potential to address one of the major challenges forecast for Moore's Law (power consumption), while the tunable critical current and the interplay between Coulomb Blockade [2] and the proximity effect [1,3] provide a platform for the study of exciting mesoscopic physics [3]. Here progress is presented towards the realisation of a nano-hybrid JOFET where two Al leads are used to form the source and drain contacts of a Si MOSFET [4]. The device is fabricated from a near-intrinsic Si substrate complemented by the use of two Al deposition steps: one for the leads and one for the gate electrode, with the gate electrode fabricated to completely overlap the source and drain. For $T < T_C$ we found the signature of disordered Andreev reflection [3] but not yet of a fully operational JOFET [1,3], however, for $T > T_C$ it was found that the device performs as a p-MOS Schottky barrier-controlled MOSFET, as determined by the Schottky barrier at the Al-Si interface [4,5], which does not necessitate source/drain implant or diffusion. This development introduces important advantages due to the planar structure and the simple fabrication process. Furthermore, this device works as a Tunnel FET at cryogenic temperatures (< 100 K) due to the dominance of the reverse biased electrode during device operation, offering great potential for novel-nanoscale and cryogenic geometries, and, as a further advantage, compatibility with both CMOS and superconducting logic technology.

[1] A. W. Kleinsasser and T.N. Jackson, *IEEE Transactions on Magnetics* **25** 2, 1274 (1989)

[2] A. Rossi *et. al*., *Nano lett.* **14**, 3405 (2014).

[3] S. De Franceschi e*t. al*., *Nature Nanotechnol.* **5**, 703 (2010).

[4] W. Purches *et. al.*, in preparation.

[5] J. M. Larson and J. P. Snyder, *IEEE Transactions on Electron Devices* **53** 5, 1048 (2006).

Strong Eddy–Current Shielding of Ferromagnetic Resonance Response in Sub–Skin–Depth–Thick Conducting Magnetic Multilayers

I.S. Maksymov, Z. Zhang, C.S. Chang and M. Kostylev

School of Physics, M013, University of Western Australia, Crawley WA 6009, Australia.

Many magnonic and spintronic devices operate at microwave frequencies and they consist of nonmagnetic (NM) and ferromagnetic metal (FM) multilayers. It is a common belief that metal layers thinner than the microwave skin–depth do not affect the ferromagnetic resonance (FMR) response. However, the crucial role of the microwave eddy currents (ECs) in the formation of the FMR response of sub–skin–depth–thick FM films has been established theoretically [1–3]. Numerous experiments have confirmed a strong impact of ECs on the FMR response of thin FM films (see, e.g., [2]).

We investigate NM/FM/NM multilayers and present experimental evidence of a strong and adverse effect of sub–skin–depth–thick NM (Cu) capping layers on the strength and profile of the FMR response of the underlying FM (Permalloy=Py) layer. We show that ECs circulating in the capping layer shield the Py layer from the microwave magnetic field induced by the microstip line transducer of the broadband FMR spectroscopy setup [4].

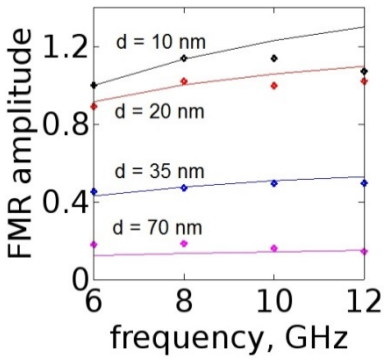

Fig. 1. Experimental (symbols) and theoretical (curves) relative amplitudes of the FMR response of the Cu–Py multilayer samples as a function of the microwave frequency. *d* denotes the thickness of the Cu capping layer facing the microstrip line transducer of the broadband FMR setup.

[1] M. Kostylev, *J. Appl. Phys.* **106**, 043903 (2009).

[2] K. J. Kennewell, M. Kostylev, N. Ross, R. Magaraggia, R. L. Stamps, M. Ali, A. A. Stashkevich, D. Greig and B. J. Hickey, *J. Appl. Phys.* **108**, 073917 (2010).

[3] I.S. Maksymov and M. Kostylev, *J. Appl. Phys.* **113**, 043927 (2013).

[4] I.S. Maksymov and M. Kostylev, invited critical review, to appear in Physica E.

WA4

The Zeeman Effect and Hyperfine Structure of a Single Erbium Ion in Silicon

C. Yin[a], M. Rancic[b], G. de Boo[a], B.C. Johnson [c], J. McCallum[c], M.J. Sellars[b] and S. Rogge[a]

[a] *Centre of Excellence for Quantum Computation and Communication Technology, School of Physics, University of New South Wales, Sydney, New South Wales 2052, Australia.*

[b] *Centre of Excellence for Quantum Computation and Communication Technology, RSPE, Australian National University, Canberra, Australian Capital Territory 0200, Australia.*

[c] *Centre of Excellence for Quantum Computation and Communication Technology, School of Physics, University of Melbourne, Melbourne, Victoria 3010, Australia.*

Erbium in silicon is one of the most appealing approaches for developing on-chip light sources, as it has the direct optical transition at 1.54 μm that is suitable for Si photonic circuits and optical fibre communication [1]. However, the optical efficiency is low till now, and one important problem is the difficulty in distinguishing or identifying different erbium sites in silicon by the site symmetry. With the single-atom spectroscopy [2], we identified individual erbium ions in silicon, and studied the Zeeman effect and hyperfine structure of a single erbium ion which are essential to figure out the site symmetry.

A single-electron transistor (SET) was used as a charge detector to observe the resonant ionization as a function of photon energy. As a result, individual erbium centres can be optically excited and electrically detected with exceptionally narrow linewidths. Individual Er centres were spectrally distinguished showing a minimum linewidth of 50 neV via the photoionisation spectroscopy [2]. In contrast, the smallest width of Er spectral lines observed in silicon had been about 8 μeV [3]. Using this technique, the Zeeman effect of individual Er centres was studied with high resolution. For the first time, the hyperfine structure of individual ^{167}Er centres in silicon was clearly shown.

[1] A.J. Kenyon, *Semicond. Sci. Technol.* **20**, R65 (2005).

[2] C. Yin, M. Rancic, G.G. de Boo, N. Stavrias, J.C. McCallum, M.J. Sellars, and S. Rogge, *Nature* **497**, 91 (2013).

[3] N.Q. Vinh, N.N. Ha, and T. Gregorkiewicz, *Proc. IEEE* **97**, 1269 (2009).

WP1

Thermodynamic Properties of a Heisenberg Model for the 'Quantum Spin-Ice' Pyrochlore $Yb_2Ti_2O_7$

J. Oitmaa[a] and R.R.P Singh[b]

[a] *School of Physics, University of New South Wales, Sydney N.S.W. 2052, Australia.*

[b] *Department of Physics, University of California, Davis, CA 95616, U.S.A.*

The rare-earth titanates $R_2Ti_2O_7$ are a series of frustrated magnetic materials, with the magnetic ions forming the 'pyrochlore' lattice, a network of corner-sharing tetrahedra.

Different members of the series show widely differing properties. The classic 'spin-ice' materials (R = Dy, Ho) have highly degenerate ground states, and no magnetic long-range order. There is much current interest in the R = Yb material, in which quantum fluctuations are much greater [1,2]. It remains controversial whether this material orders at very low temperatures, or whether its ground state is an example of the rather elusive 'quantum spin-liquid' phase.

A model for $Yb_2Ti_2O_7$ has been proposed, and its parameters estimated by fitting to inelastic neutron scattering data [1]. This is an anisotropic spin S=1/2 Heisenberg model with four kinds of exchange term. An analysis via linear spin-wave and mean-field methods has been reported and used in the parameter fitting. However, these methods are not always reliable.

In the present work we perform a more precise analysis of this model, using high-temperature series expansions [3]. The results are in good agreement with experimental specific heat and susceptibility data

[1] K.A. Ross, L. Savary, B.D. Gaulin and L. Balents, *Phys. Rev. X* **1**, 021002 (2011).

[2] H. Yan, O. Benton, L. Jaubert and N. Shannon, *arXiv:* 1311.3501 (2013).

[3] J. Oitmaa, C.J. Hamer and W.-H. Zheng, *Series Expansion Methods for Strongly Interacting Lattice Models* (Cambridge University Press Press, 2006) .

WP2

Complementary Raman and Mössbauer Archaeological Studies

John D. Cashion[a] and William H. Jay[b,c]

[a] *School of Physics, Monash University, Melbourne 3800, Australia.*

[b] *Private Researcher, P.O. Box 34, Chelsea, 3196, Australia.*

[c] *Centre for Archaeology and Ancient History, Monash University, Melbourne 3800, Australia.*

Archaeological investigations often proceed by a mixture of extensive careful digging and searching followed by physical and scientific examination and comparisons with previous related samples. In common with all scientific investigations, they build on previous work. However, as with works of art, there is often reliance on connoisseurship to certify that a particular item can be attributed to a certain provenance. Proving, or disproving, such assertions can involve much detailed scientific analysis.

Archaeological investigations can provide much useful knowledge on the state of technological capability at that time and place, the development and transfer of technology, trade routes and so on. We have been carrying out investigations on Egyptian artifacts from the Dakhleh Oasis from circa 18th dynasty and earlier (3300+ years ago) and 18th century Limehouse porcelain and Lancaster delftware as they developed their clays and glazes.

Using two different spectroscopies produces a much more detailed picture. For example, one item of particular interest is the firing temperature available at that time. Raman is able to identify the minerals in the body and the glazes and, from knowledge of the formation and transformation temperatures of the minerals, deduce the minimum temperature and also that other temperatures were not reached. The Lancaster pottery was largely made from local clay mixed 1:1 with dolomitic clay from Carrickfergus near Belfast, which was only available at the time at low tide and has now been covered by sea defences. Combined with the Mössbauer analysis we deduce that the firing temperature was between 900 and 990°C. The various pigments and glazes often had traceable unique origins in Europe.

Mössbauer analysis of an Egyptian slag showed the iron content to be a goethite and aluminosilicate mixture in the centre but pure goethite on the surface with single crystals up to 5mm in length from dissolution and recrystallisation over 3000 years. Spectra of the surface and centre of a pottery sherd showed that the firing was inadequate to transform the material through to the centre.

WP3

Avalanche Behaviour at First-Order Phase Transitions

T.R. Finlayson[a] and J.C. Lashley[b]

[a] *School of Physics, University of Melbourne, Victoria 3010, Australia.*

[b] *Los Alamos National Laboratory, Los Alamos, U.S.A.*

Across the physical and biological sciences one can find many examples of changes in a system, which are controlled by fluctuations or critical-point behaviour and for which Ball has used the expression "at the edge of chaos" [1]. Phenomena ranging from the statistics of molecules to seismic disturbances have been shown to exhibit critical-point fluctuations of the form, $P(E) \propto E^{-\varepsilon}$, where $P(E)$ is the probability of finding an avalanche with energy, E [2].

First-order phase transitions in condensed matter are an example of one such natural phenomenon and there are now many examples of the measurement of noise spectra in association with first-order phase transitions and the analyses of pulse amplitudes and pulse durations, according to the above expression. One specific example is the martensitic transformation for which the best accepted definition is "a cooperative motion of a set of atoms across an interface causing a shape change and sound" [3]. Indeed, the measurement of noise spectra using acoustic emission has often been the technique applied to illustrate avalanche behaviour for the example of the first-order martensitic transition [4]. But acoustic emission is not the only physical property for which noise spectra have been observed [5].

In this paper the results from some of this research will be reviewed. Our own recent research on the A15-structure compound, V_3Si, which exhibits a martensitic transition just a few degrees above its superconducting critical temperature of 17 K will be summarized.

[1] P. Ball, *New Scientist*, **222**, (2966) 44 (2014).

[2] M.B. Weissman, *Rev. Mod. Phys.* **60**, (2) 537 (1988).

[3] P.C. Clapp, in *ICOMAT 95 – International Conference on Matensitic Transformations, Part I* eds. R. Gotthardt and J. Van Humbeeck, *J. de Physique (Colloque C8) suppl. J. de Physique III* **5,** C8-11 (1995).

[4] M.C. Gallardo, J. Manchardo, F.J. Romero, J. del Carro, E.K.H. Salje, A. Planes, E. Vives, R. Romero and M. Stipeich, *Phys. Rev. B* **81,** 174102-1 (2010).

[5] J.C. Lashley, K. Gofryk, B. Milhaila, J.L. Smith and E.K.H. Salje, *J. Phys.: Condens. Matter* **26,** 035701 (2014).

WP4

First-order magnetic phase transition in TmGa

J.M. Cadogan[a] and M. Avdeev[b]

[a] *School of Physical, Environmental and Mathematical Sciences, UNSW Canberra at the Australian Defence Force Academy, Canberra, ACT, BC 2610, Australia.*

[b] *Bragg Institute, Australian Nuclear Science and Technology Organisation, PMB 1, Menai, NSW 2234, Australia.*

In a recent paper [1] we determined the magnetic structure of the intermetallic compound TmGa using a combination of neutron diffraction and ^{169}Tm Mössbauer spectroscopy. This compound shows two magnetic 'events' in its ac-susceptibility, at 15(1) K and 12(1) K. The upper transition is to an incommensurate antiferromagnetic structure which gives way to a dominant ferromagnetic structure at the lower transition. However, the Mössbauer results suggested that the 12 K transition is in fact first-order.

In order to resolve this question, we have carried out a high-resolution, neutron diffraction thermal scan around these magnetic ordering events and we have observed clear thermal hysteresis in the behaviour of the magnetic scattering intensity. The observation of such hysteresis confirms our earlier suggestion of a first-order magnetic ordering in TmGa.

[1] J.M. Cadogan, G.A. Stewart, S. Muñoz Pérez, R. Cobas, B.R. Hansen, M. Avdeev and W.D. Hutchison, *J. Phys. Condensed Matter* **26**, 116002 (2014).

Residual microstructure effects of mobile bismuth surface droplets formed during molecular-beam-epitaxy of GaAsBi

J.A. Steele[a], R.A. Lewis[a], M. Henini[b], O.M. Lemine[c], D. Fan[d,e], Yu. I. Mazur[e], V.G. Dorogan[e], P.C. Grant[d], S.-Q. Yu[d,e] and G.J. Salamo[e]

[a] *Institute for Superconducting and Electronic Materials, University of Wollongong, Wollongong, New South Wales 2522, Australia.*

[b] *School of Physics and Astronomy, Nottingham Nanotechnology and Nanoscience Center, University of Nottingham, Nottingham NG7 2RD, United Kingdom.*

[c] *Department of Physics, College of Sciences, Al Imam Muhammad Ibn Saud Islamic University (IMSIU), Riyadh, 11623 Riyadh, Saudi Arabia.*

[d] *Department of Electrical Engineering, University of Arkansas, Fayetteville, AR, 72701, USA*

[e] *Institute for Nanoscience and Engineering, University of Arkansas, Fayetteville, AR 72701, USA.*

We report the residual effects of high-mobility metallic bismuth surface droplets formed during the molecular-beam-epitaxy of (100) GaAsBi [1]. Surface modifications introduced through surface droplet formation are characterised by employing a combination of electron microscopy and micro-optical techniques, revealing significant changes in the structural and optical properties of the surface semiconductor. Namely, Bi droplets appear to move across the surface during growth and display a raised ``track'' following the droplet path, ending with a small micro-disc structure formed through vapor-liquid-solid mechanisms. Raman scattering measurements [2,3] reveal a high level of disorder within the track path and a substantial bandgap energy increase from light emitted from the GaAsBi micro-discs. We discuss the mechanisms of Bi droplet migration and subsequent formation of new microstructures, and conclude that while droplet removal - through selective chemical wet etch techniques - appears to rid the bismuth bulk, the residual effects on the epitaxial layer are substantial and cannot be overlooked.

[1] J.A. Steele and R. A. Lewis, *Opt. Express* **22**, 32261-32275 (2014).

[2] J.A. Steele, R.A. Lewis, M. Henini, O.M. Lemine and A. Alkaoud, *J. Appl. Phys.* **114**, 193516 (2013).

[3] J.A. Steele, R.A. Lewis, M. Henini, O. M. Lemine, D. Fan, Yu. I. Mazur, V. G. Dorogan, P.C. Grant, S.-Q. Yu and G.J. Salamo, *Opt. Express* **22**, 11680-11689 (2014).

WP6

Spin splitting of heavy holes in magnetic focusing experiments

S. Bladwell and O. P. Sushkov

School of Physics, University of New South Wales, NSW 2052, Australia.

The dynamics of charge carriers in low dimensional heterostructures subject to spin-orbit interactions has presented a wide variety of novel phenomena, and potential applications, for instance, spintronics. In this work, we investigate theoretically heavy-holes magnetically focused via a weak transverse magnetic field in a zinc-blende two-dimensional semiconductor heterostructure. In systems like this the spin-orbit interaction, in particular Rashba spin-orbit interaction, can be a significant fraction of the Fermi energy. This strong spin-orbit splitting leads to a double peak in the magnetic focusing spectrum. A several tesla magnetic field is applied in-plane, the result is a hole-density-dependent Zeeman splitting suppressing or enhancing the spin-split focusing peaks. From this analysis we present predictions for experiments.

WP7

The Lifetime of Magnons in the Vicinity of Quantum and Thermal Phase Transitions

H.D. Scammell and O.P. Sushkov

School of Physics, University of New South Wales, NSW 2052, Australia.

The zero temperature quantum phase transition between the disordered and ordered phases of a three-dimensional quantum antiferromagnet is identified with the spontaneous breakdown of O(3) spin rotational symmetry. The disordered phase is described by three gapped magnetic excitations (magnons), while the symmetry broken ordered phase is described by two gapless Goldstone excitations and one gapped Higgs excitation. The disordered phase can be restored by thermally driving the ordered phase above the Neel temperature. This is the thermal phase transition.

We seek a complete description of the quantum and thermal phase transitions of the system in one unifying framework. Starting from an effective field theory, we use thermalised Greens functions to obtain; the Neel temperature curve; the temperature dependence of the gap of the magnons in each phase; the spectral intensity of the magnons; and finally their lifetimes. We compare our results with the recent experimental data obtained for the compound $TlCuCl_3$ and find excellent agreement.

WP8

The Frequency-dependent Seismic Properties of Cracked and Fluid-saturated Glass-bead Media

Y. Li[a], E.C. David[a], I. Jackson[a] and D.R. Schmitt[b]

[a] *Research School of Earth Sciences, ANU, Canberra, ACT, Australia.*

[b] *Department of Physics, University of Alberta, Edmonton, AB, Canada.*

The expected frequency dependence of seismic wave velocities in cracked and fluid-saturated crustal rocks complicates the use of laboratory velocity measurements, traditionally limited to MHz frequencies, for interpretation of seismic data collected at lower frequencies. For appropriately low frequencies of wave propagation, such dispersion results from the relaxation of spatial gradients in pore-fluid pressure by fluid flow. The solution to this dilemma lies in laboratory measurements of elastic velocities, or corresponding moduli, over an appropriately wide range of frequencies. To this end, conventional measurements with ultrasonic (MHz) wave propagation methods are being complemented by sub-resonant forced-oscillation techniques that provide access to lower frequencies. Ultrasonic measurements of P and S wave velocities, and forced-oscillation measurements in both torsional and flexural modes at low frequencies (MHz-Hz), have been conducted on a series of soda-lime silica glass samples with porosities varying from 0 to 6%. Samples were prepared either from dense glass rod or by sintering glass beads under controlled conditions, and subjected to subsequent thermal cracking. All samples are successively tested dry, and with argon and water as pore fluids. The results show systematic increases in wave velocities or elastic moduli with increasing differential pressure (confining pressure minus pore pressure) – interpreted in terms of crack closure. Fluid saturation, especially with water, results in a substantial increase in the moduli measured at MHz frequencies - evidence that the ultrasonic technique is sampling the saturated isobaric regime. A micromechanical model, based on Eshelby's results and using the differential effective medium scheme, yields crack aspect ratios and crack density as functions of pressure, as well as providing theoretical estimates of the effect of saturation and frequency on elastic moduli. Such dispersion between Hz and MHz frequencies needs to be taken into account in seismological applications of laboratory wave-speed measurements.

WP9

Magnetic ordering in $Er_2Fe_2Si_2C$ and $Tm_2Fe_2Si_2C$

R.A. Susilo[a], J.M. Cadogan[a], W.D. Hutchison[a], M. Avdeev[b], D.H. Ryan[c], T. Namiki[d] and S.J. Campbell[a]

[a] *School of Physical, Environmental and Mathematical Sciences, UNSW Canberra at the Australian Defence Force Academy, Canberra BC, ACT 2610, Australia.*

[b] *Bragg Institute, ANSTO, PMB 1, Menai, NSW 2234, Australia.*

[c] *Department of Physics, McGill University, Montreal, QC H3A 2T8, Canada.*

[d] *Graduate School of Science and Engineering, University of Toyama Gofuku, Toyama, 930-8555, Japan.*

The magnetic ordering of two members of the $R_2Fe_2Si_2C$ (R = rare-earth) series of compounds (monoclinic $Dy_2Fe_2Si_2C$-type structure with the *C2/m* space group), $Er_2Fe_2Si_2C$ and $Tm_2Fe_2Si_2C$, have been studied by neutron powder diffraction and ^{166}Er Mössbauer spectroscopy, complemented by magnetisation and specific heat measurements. In both cases, antiferromagnetic ordering of the R sublattice is observed, with Néel temperatures of 4.8(2) K and 2.6(3) K for $Er_2Fe_2Si_2C$ and $Tm_2Fe_2Si_2C$, respectively. The magnetic structures of the Er- and Tm-based compounds are quite different from those found for the other members of the $R_2Fe_2Si_2C$ series. Previous studies show that the common magnetic structure of the heavy-$R_2Fe_2Si_2C$ compounds involves ordering of the R sublattice along the b-axis with a propagation vector **k** = [0, 0, ½] [1, 2]. However, the antiferromagnetic structure of the Er sublattice in $Er_2Fe_2Si_2C$ is described by **k** = [½, ½, 0] with the Er magnetic moments lying close to the ac-plane. $Tm_2Fe_2Si_2C$ is found to exhibit a more complex magnetic structure that is characterised by a square-wave modulation of the Tm magnetic moments along the a-axis and a cell-doubling along the b-axis with **k** = [0.403(1), ½, 0]. The differences in the magnetic structures of these compounds are interpreted in terms of the RKKY exchange interaction, which depends on the R-R interatomic distances, and crystal field effects acting on the R^{3+} ions.

[1] J. Le Roy, D. Paccard, C. Bertrand, J.L. Soubeyroux, J. Bouillot, L. Paccard and D. Schmitt, *Solid State Commun.*, **86**, 675 (1992).

[2] R.A. Susilo, J.M. Cadogan, R. Cobas, W.D. Hutchison, M. Avdeev and S.J. Campbell, *J. Appl. Phys.* (accepted).

WP10

Non-ergodicity in Praseodymium Oxide

J.R. Sellar

Department of Materials Engineering, Monash University, Clayton, Victoria 3800, Australia.

The α-phase of Praseodymium Oxide appears to violate the normal tenets of equilibrium thermodynamics in tensimetric experiments, in particular Gibbs' Phase Rule. Isoplethic (equal concentration) replots of data from isobaric (equal pressure) experiments were found to display four "pseudophases" in the α region instead of one. The opposite experiments – isobaric replots of isoplethic data – also revealed four unexpected phases. Neither of the two types of direct experiment (isoplethic or isobaric) exhibit any such subdivision of the α-phase into four subphases, but the four pseudophases revealed in each of the two derived plots, however, do not appear to be the same. This unusual behavior is suggested to be due to existence of several "invariant equilibrium states", which lead directly to the violation of the Phase Rule and arise from the ergodic breakdown of the supposedly single disordered α-phase into four pseudophases, each displaying strong memory effects.

Spin-spiral to spin-stripe phase transition driven by fluctuations

A.I. Milstein[a] and O.P. Sushkov[b]

[a] *Budker Institute of Nuclear Physics of SB RAS, Novosibirsk, 630090, Russia.*

[b] *School of Physics, University of New South Wales, NSW 2052, Australia.*

We consider behavior of spin spiral systems in the vicinity of a critical point separating the spin ordered and the spin disordered states. We demonstrate that generically the critical point splits in two close but separate critical points. In the first one the spin spiral is transformed to the spin stripe, and in the second point the spin ordering disappears altogether. Specifically we address $TbMnO_3$ multiferroic and cuprate superconductors.

WP12

Magnetic Structure of $TbRu_2Al_{10}$

R. White[a], W.D. Hutchison[a] and T. Mizushima[b]

[a] *School of Physical, Environmental and Mathematical Sciences, The University of New South Wales, Canberra ACT 2600, Australia.*
[b] *Graduate School of Science and Engineering, University of Toyama, Toyama, Japan.*

The rare earth intermetallic compound $TbRu_2Al_{10}$ forms with the orthorhombic *$YbFe_2Al_{10}$* structure type [1] in the space group Cmcm (#63). Related iron type materials that crystallise with the same structure have shown interesting magnetic properties when cooled to low temperature [2,3] including an incommensurate magnetic phase best described as a 'zigzag' antiferromagnet. Magnetometry and heat capacity measurements indicate a magnetic transition at 15 K for $TbRu_2Al_{10}$. Recent powder neutron diffraction studies on $TbRu_2Al_{10}$ have revealed that it forms an incommensurate magnetic structure with a propagation vector of $\boldsymbol{k}$ = (0, 0.759(1), 0) below the ordering temperature, with the largest magnetic moment equal to 7.7(1) μ_B at 6 K. This magnetic structure is sinusoidally modulated along the *b*-axis direction and is slightly different to that observed in the iron analogue, while maintaining an overall zigzag antiferromagnetic character.

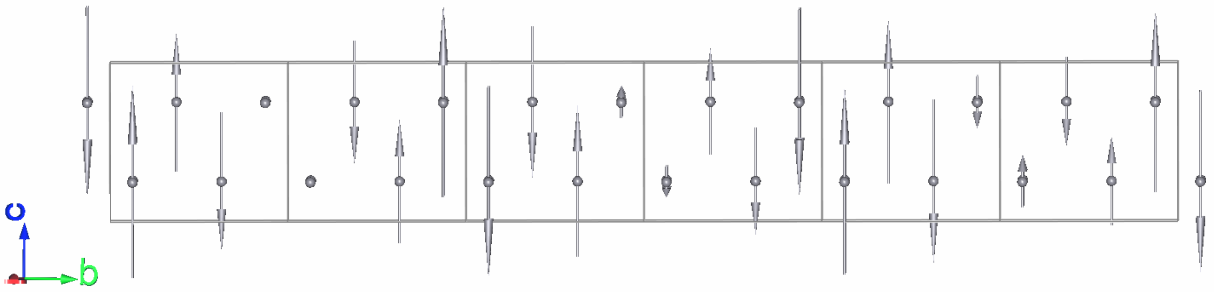

Figure 1: Six unit cells of $TbRu_2Al_{10}$ viewed down the *a*-axis showing the sinusoidal nature of the Tb^{3+} magnetic moment at 6 K. Other atoms in the unit cell have been excluded for clarity.

[1] V.M.T. Thiede, T. Ebel and W. Jeitschko, *J. Mater. Chem.* **8**(1), 125-130 (1998).

[2] M. Reehuis, B. Fehrmann, M.W. Wolff, W. Jeitschko and M. Hofmann, *Physica B* **276–278**(1), 594-595 (2000).

[3] M. Reehuis, M.W. Wolff, A. Krimmel, E.W. Scheidt, N. Stüsser, A. Loidl and W. Jeitschko, *J. Phys: Condens. Matter* **15**(10), 1773 (2003).

Spin-charge separation in 2D: magnetization density induced by spin 1/2 impurity in the vicinity of quantum critical point

Y. Kharkov, I. Terekhov and O. Sushkov
School of Physics, University of New South Wales, NSW 2052, Australia.

Spin-charge separation (SCS) is an unusual phenomenon in some materials that results in spatial separation of charge and spin degrees of freedom of fermions. SCS was discovered for the first time in one dimensional systems of strongly interacting electrons [1, 2]. The existence of the SCS phenomenon in two dimensional (2D) systems was proven later on [3]. One of examples of such systems that exhibit SCS in 2D is antiferromagnets in the vicinity of the quantum critical point (QCP), dividing the phase diagram between magnetically ordered and disordered phases [4, 5]. When a magnetic impurity is added to such systems, the spin of the impurity delocalises in a divergent magnon cloud with a radius $R\sim 1/\Delta$, where Δ is the magnon gap of excitations in the disordered phase. In the present work we consider spatial distributions of spin density induced by a spin ½ immobile impurity. On example of the bilayer antiferromagnet model with $O(3)$ quantum critical point, we find the spatial distribution of spin density has the power-law form $Z/r^{3/2}$ at distances much greater than the lattice spacing and smaller than the inverse magnon gap. Here Z is a constant of renormalisation of the impurity spin and at the QCP, $Z \to 0$ that provides the necessary condition for SCS. We show that at the critical point the total spin of the impurity is carried by a magnon field and is equal to 1/2.

[1] S.I. Tomonaga, *Prog. Theor. Phys.* **5**, 544 (1950)
[2] J.M. Luttinger, *J. Math. Phys.* **4**, 1154 (1963).
[3] W.O. Putikka, R.L. Glenister, R.R.P. Singh and H. Tsunetsugu, *Phys. Rev. Lett.* **73**, 170 (1994).
[4] O.P. Sushkov, *Phys. Rev. B* **62**, 12135 (2000).
[5] M. Holt, J. Oitmaa, W. Chen and O.P. Sushkov, *Phys. Rev. B* **87**, 075109 (2013).

WP14

The Apparent Neglect of the Effects on 'Winehealth', and in Wines, of 'Radical Ions'

G.J.Troup[a] and S. Drew[b]

[a] *School of Physics, Monash University, Victoria 3800, Australia.*

[b] *Florey Department of Neuroscience and Mental Health, University of Melbourne, Victoria 3010, Australia.*

'Radical ions' is an old name for transition metal ions. Cu2+, Mn2+ and Fe3+ , all occurring in wines, are clearly antioxidants.'Winehealth' Cu2is the health giving/protecting effects of wine in moderation. Cu2+ is a part of SOD1, and Mn2+ is not only necessary for SOD2, but has a chaperone molecule. These two ions are known to interact with polyphenols. Cu2+ is used in many 'model wines' which usually contain catechin, and contain free radicals. Mn2+ used in a model wine with quercitin shows free radicals also, and is slightly fluorescent. Is this the cause of the fluorescence seen in some white wines? Many papers are written about the different content of polyphenols in wines from different districts, but how many have been written about the different effects of different concentrations of these two ions, for example? It is known that treating the vines with a Mn compound at the appropriate time will increase flowering: this must affect wine quality, and even perhaps polyphenol content. Other effects due to changes in Cu content will be dealt with in the paper, which is intended to stimulate research in these areas, and not to forget the radical ions!

WP15

The Magnetic Ground State of Dy^{3+} in $DyNiAl_4$

W.D. Hutchison, G.A. Stewart and J.M. Cadogan

School of Physical, Mathematical and Environmental Sciences,

The University of New South Wales, Canberra, ACT 2600, Australia.

The orthorhombic, intermetallic series $RNiAl_4$ (R = rare earth) exhibits a range of interesting magnetic behaviour [1 & refs therein], including the potential for low temperature, inverse, magnetic cooling [2,3]. Earlier specific heat measurements in zero applied field on polycrystalline $DyNiAl_4$ revealed phase transitions at T_N = 18 K and T_N' = 15 K [3]. Following trends observed in the $RNiAl_4$ series, it is expected that the Dy sub-lattice orders with an incommensurate magnetic structure at ~18 K and to commensurate antiferromagnetism at ~15 K. The low temperature magnetisation curve showed metamagnetic transitions near 2.5 T and 6.25 T. However, at the maximum applied field of 9 T the bulk magnetisation of 4.7 μ_B/f.u. is only near half of the maximum free-ion moment of 10 μ_B/Dy^{3+} ion [3]. It was uncertain whether crystal field quenching was responsible for a reduced local Dy^{3+} magnetic moment or whether increased applied fields were needed to overcome the large magnetocrystalline anisotropy. In this present investigation the two transition temperatures are confirmed using magnetic susceptibility measurements and the inverse paramagnetic susceptibility is observed to follow Curie-Weiss behaviour with an effective Dy^{3+} moment of μ_{eff} = 10.7(1) μ_B/Dy^{3+}. This is in excellent agreement with the Dy^{3+} free-ion value of 10.65 μ_B/Dy^{3+}. The magnetic ground state of Dy^{3+} in $DyNiAl_4$ has also been probed using low temperature ^{161}Dy Mössbauer spectroscopy which has the advantage of being a zero applied field measurement. Using Dy metal [4] as the calibration reference, the magnetic hyperfine field at the ^{161}Dy nucleus in $DyNiAl_4$ is 548(3) T at 5 K. Compared with the free-ion field of 559.8 T, this implies a local Dy^{3+} moment of 9.8 μ_B which is close to the full free-ion moment of 10 μ_B and rules out the possibility of significant crystal field quenching.

[1] W.D. Hutchison, D.J. Goossens, K. Nishimura, K. Mori, Y. Isikawa and A.J. Studer, *J. Magn. Magn. Mater.* **301**, 352-358 (2006).

[2] L. Li, K. Nishimura and W.D. Hutchison, *Solid State Commun.* **149**, 932-936 (2009).

[3] W.D. Hutchison, N. Segal and K. Nishimura, Proceedings of the 36th Annual Condensed Matter and Materials Meeting, Wagga Wagga, WP14: p1-4 (2012).

[4] Y. Berthier and J. Barak, *Solid State Commun*. **17**, 153-155 (1975).

Synchrotron Powder Diffraction Investigations of the Crystal Structure of the Solid Solution $Cu_{1-x}Co_xSb_2O_6$

H.-B. Kang[a], T.R. Finlayson[b] and T. Söhnel[a]

[a] *School of Chemical Sciences, University of Auckland, Auckland, New Zealand.*

[b] *School of Physics, University of Melbourne, Victoria 3010, Australia.*

$CuSb_2O_6$ is the most intensively studied compound in the ternary Cu-Sb-O system. It shows a second order phase transition from tetragonal trirutile to monoclinic trirutile structure as Cu^{2+} (d^9 system) forms the square lattice oxide layer, which leads the second order phase transition (Jahn-Teller distortion) [1]. $CoSb_2O_6$ crystallises in tetragonal trirutile structure [2]. The systematic reduction in symmetry would require the existence of an orthorhombic modification between the two modifications. From synchrotron high temperature measurements, the phase transition can be clearly observed and a possible orthorhombic modification (*Pnnm*) can be refined from 200°C data. Measurements from 25°C to 900°C show the negative thermal behaviour (Fig. 1, right). Rietveld refinements of $CuSb_2O_6$ also show the appearence of domain wall effects. Domain walls are characterised by the discrete symmetry being spontaneously broken resulting in a broadening of the Bragg peaks in the powder pattern (Fig. 1, left).

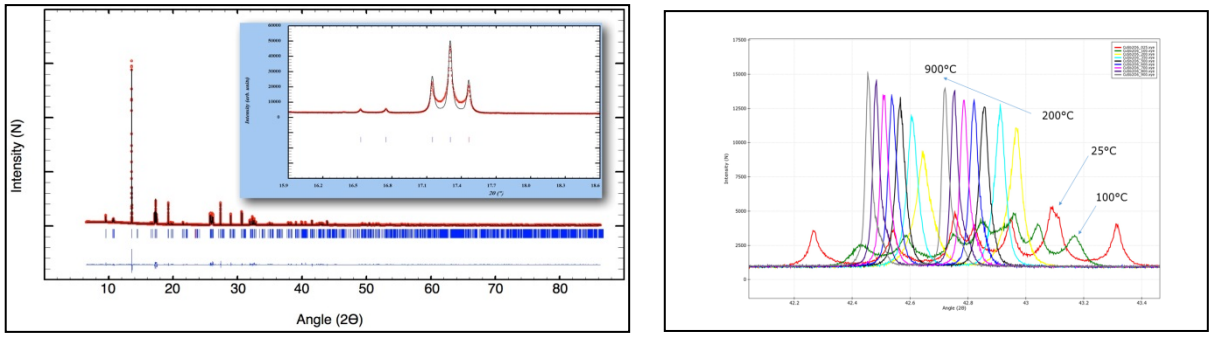

Fig 1. Rietveld refinement of $CuSb_2O_6$ on synchrotron powder data at 25ºC (left); high-temperature measurements of $CuSb_2O_6$ between 25ºC and 900ºC.

[1] A.V. Prokofiev, F. Ritter, W. Assmus, B.J. Gibson and R.K. Kremer, *J. Cryst. Growth*. **247**, 457 (2003).

[2] J.N. Reimers, J.E. Greedan C.V. Stager and R. Kremer, *J. Solid State Chem.* **83**, 20 (1989).

THURSDAY ABSTRACTS

Semi-classical orbits of phosphorus donors in silicon under a magnetic field

A. Bruno-Alfonso[a], C. Bleasdale[b], G.V.B. de Souza[a] and R.A. Lewis[b]

[a] *School of Science, São Paulo State University, SP 17033360, Brazil.*

[b] *School of Physics, University of Wollongong, NSW 2522, Australia.*

The manifestation of semi-classical orbits of an electron in the optical spectrum of a hydrogen atom in a magnetic field has been studied experimentally and theoretically in the 1980's [1,2]. According to the effective-mass theory, shallow donor impurities in semiconductor materials should display a similar dynamics. In 2009, Chen *et al*. [3] have found experimental evidence of this by photothermal ionisation spectroscopy of a phosphorus-doped silicon sample, with 10^{11} impurities per cubic centimeter, at 17 K. However, the anisotropy of the effective mass in each valley of the conduction band of silicon poses new theoretical challenges. By numerically solving the equations of motion, we have shown that the shape and duration of the main closed orbits depend on the magnetic-field direction [4]. When the field is applied along the main directions of the silicon crystal, the periods have been found in good agreement with the experimental data reported by Chen *et al*. [3]. Additionally, a discussion on the appropriate experimental conditions for the manifestation of the semi-classical orbits in the optical spectrum of silicon and other semiconductor materials is presented.

[1] J. Main, G. Wiebusch, A. Holle and K.H. Welge, *Phys. Rev. Lett.* **57**, 2789 (1986).

[2] M.L. Du and J. B. Delos, *Phys. Rev. A* **38**, 1896 (1988).

[3] Z. Chen, W. Zhou, B. Zhang, C.H. Yu, J. Zhu, W. Lu and S. C. Shen, *Phys. Rev. Lett.* **102**, 244103 (2009).

[4] A. Bruno-Alfonso, C. Bleasdale, G. V. B de Souza and R. A. Lewis, *Phys. Rev. A* **89**, 043425 (2014).

TM2

Elasticity of lizardite-1T from dispersion-corrected DFT

R. Skelton

Research School of Earth Sciences, Australian National University, Canberra 2601, Australia.

Hydrous minerals are abundant throughout the Earth's Crust, and strongly influence its structure and rheology. They are particularly common in oceanic crust, and the dehydration of hydrous minerals during subduction is the principal mechanism by which water is transported into the mantle. Many hydrous minerals have a layered structure, with the layers held together by hydrogen bonding or van der Waals interactions. This complicates attempts to model their properties using density functional theory (DFT), which neglects long ranged, dispersive contributions to the total energy. The DFT-D2 scheme [1], in which an empirical dispersion term C_6r^{-6} is added to the energy of the simulation cell, is widely used to model dispersion forces in DFT calculations. However, DFT-D2 was developed for covalently-bonded molecules and, consequently, significantly underestimates the cell parameters of ionic solids. Here, we show that a simple, empirically-motivated re-parametrisation of the DFT-D2 model, using experimental values for the ionisation energy, free ion polarisability, and crystal radius of each ionic species, provides close agreement between experimental and theoretical properties of hydrous minerals. As an example, we use the new parameter set to calculate the crystal structure and elastic constants of the serpentine mineral lizardite-1T, $Mg_3Si_2O_5(OH)_4$, to mantle pressures. Compared with calculations performed with the dispersion coefficients in [1], the DFT-D2 parameters proposed in this study provide a much closer fit to experimental cell volume data [3]. On the basis of dispersion-uncorrected DFT calculations, a previous study predicted that the compression mechanism of the lizardite-1T *c*-axis changes at pressures approaching 10 GPa [2]. In contrast, our calculations suggest that this transition occurs at ~4.5 GPa, within the established pressure-stability field of lizardite-1T and related serpentine minerals.

[1] S Grimme, *J. Comput. Chem.* **27**, 1787 (2006).

[2] J. Tsuchiya, *Am. Mineral.* **98**, 2046 (2013).

[3] N. Hilairet, I. Daniel and B. Reynard, *Phys. Chem. Miner.* **33**, 629 (2006).

Exploring the Properties of Mixed Cobalt/Iron/Manganese-Tin Clusters

M. Allison[a,b], C. Ling[b], G. Stewart[c] and T. Söhnel[a]

[a] *School of Chemical Sciences, University of Auckland, New Zealand.*

[b] *School of Chemistry, University of Sydney, NSW, Australia.*

[c] *School of PEMS, UNSW@AFDA, Canberra, Australia.*

Layered oxides containing third row transition metals are well known candidates for materials that exhibit novel multiferroic properties such as ferroelectricity and giant magnetoresistance. The parent compound for this presentation $Fe_4Si_2Sn_7O_{16}$ [1] provides a novel situation in oxide compounds. It can be described as a composite of intermetallic ($FeSn_6$) clusters and (FeO_6)/(SnO_6) oxide layers within the one structure. SiO_4 tetrahedra separate these layers which leads to electronic and magnetic isolation of the repeated layers by about 7 Å resulting in a nearly perfectly 2D oxide system comparable to a one layer thick oxide "thin film". This combination of features therefore allows us a unique opportunity to study the electronic interaction of two materially independent features in the one material. In this study we have replaced iron positions with cobalt and/or manganese in order to study the change in structure and material properties. Refinements of the structures from X-ray and neutron powder diffraction patterns determined changes in lattice parameters which show that the MSn$_6$ octahedral layer in these materials contain both iron and cobalt resulting in the first 19 electron cluster seen in the tin system. ^{57}Fe-Mössbauer spectra (Fig. 1) confirm the observation from neutron diffraction studies that Mn has a strong preference to sitting in the oxide layers, whereas Co preferably occupies the Sn cluster layer. In this presentation we will show the current results of our studies on the crystal and electronic structures of this family of compounds.

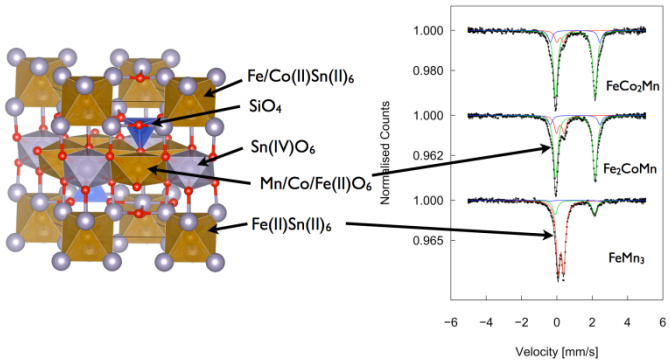

Figure 1. Crystal structure (left) and ^{57}Fe Mössbauer spectra of $Fe_{4-x-y}Mn_xCo_ySi_2Sn_7O_{16}$.

[1] T. Söhnel, P. Böttcher, W. Reichelt and F. E. Wagner, *Z. Anorg. Allg. Chem.* **624**, 708 (1998).

Effects of ^{18}O isotope substitution in multiferroic $RMnO_3$ (R=Tb, Dy)

P.J. Graham[a], N. Narayanan[b,c], N. Reynolds[a,c,e], F. Li[b], P. Rovillain[a,c], M. Bartkowiak[b,c], J. Hester[c], J. Kimpton[d], M. Yethiraj[c], E. Pomjakushina[e], K. Conder[e], M. Kenzelmann[e], G. McIntyre[c], W.D. Hutchison[b] and C. Ulrich[a,c]

[a] *School of Physics, University of New South Wales, New South Wales 2052, Australia.*

[b] *School of PEMS, UNSW Canberra, Canberra, ACT 2600, Australia.*

[c] *The Bragg Institute, ANSTO, Lucas Heights, NSW 2234, Australia.*

[d] *Australian Synchrotron, Melbourne, VIC 3168, Australia.*

[e] *Paul Scherrer Institute, CH-5232 Villigen, Switzerland.*

Multiferroic materials demonstrate desirable attributes for next-generation multifunctional devices as they exhibit coexisting ferroelectric and magnetic orders. In type-II multiferroics, coupling exists that allows ferroelectricity to be manipulated via magnetic order and vice versa, offering potential in high-density information storage and sensor applications. Despite extensive investigations into the subject, questions of the physics of magnetoelectric coupling in multiferroics remain, and competing theories propose different mechanisms. The aim of this investigation was to study changes in the statics and dynamics of structural, ferroelectric and magnetic orders with oxygen-18 isotope substitution to shine light into the coupling mechanism in multiferroic RMnO$_3$ (R=Tb, Dy) systems.

We have performed Raman spectroscopy on ^{16}O and ^{18}O-substituted TbMnO$_3$ single crystals. Oxygen-18 isotope substitution reduces all phonon frequencies significantly. However, specific heat measurements determine no changes in Mn^{3+} (28 and 41 K) magnetic phase transition temperatures. Pronounced anomalies in peak position and linewidth at the magnetic and ferroelectric phase transitions are seen. While the anomalies at the sinusoidal magnetic phase transition (41 K) are in accordance to the theory of spin-phonon coupling, further deviations develop upon entering the ferroelectric phase (28 K). Furthermore, neutron diffraction measurements on ^{16}O and ^{18}O-substituted DyMnO$_3$ powders show structural deviations at the ferroelectric phase transition (17 K) in the order of 100 fm. These results indicate that the structure is actively involved in the emergence of ferroelectricity in these materials.

TM5

Structural properties of the Nb-doped bismuth oxide materials, $Bi_{1-x}Nb_xO_{1.5+x}$

M.L. Tate, [a,b] J. Hack,[b,c] X. Kuang,[b] G.J. McIntyre, [a] R.L. Withers,[d] M.R. Johnson[c] and I.R. Evans[b]

[a] *ANSTO, Lucas Heights NSW 2234, Australia.*

[b] *Dept. of Chemistry, University of Durham, Science Site, South Road, Durham DH1 3LE, UK*

[c] *Institut Laue-Langevin, Grenoble, France.*

[d] *Research School of Chemistry, Australian National University, Canberra, Australia.*

Oxide ion conductors are used in a wide variety of applications, including oxygen sensors and separation membranes, but are undergoing significant study for their use in solid oxide fuel cells (SOFCs), which allow for the direct conversion of chemical to electrical energy.

Bismuth oxide (Bi_2O_3) exists in five polymorphs, and possesses excellent oxide ion conductivity when in the cubic fluorite structure type, due to its intrinsic oxide ion vacancies. However, this cubic structure is only stable over a small high-temperature range. Introducing niobium into the bismuth oxide structure stabilises the highly conductive cubic and tetragonal phases to room temperature, allowing for high oxide ion conductivity at lower temperatures. In addition to stabilising the high temperature structure types, doping with niobium also introduces interstitial oxygen atoms into the material in order to maintain a charge balance.
Niobium-doped bismuth oxide samples, $Bi_{1-x}Nb_xO_{1.5+x}$ (x = 0.0625, 0.12), were synthesised by a solid state synthetic method, before undergoing AC impedance spectroscopy experiments to study their electrical properties. Both samples showed excellent oxide ion conductivities, with the cubic sample (x = 0.12) possessing higher conductivity values than the tetragonal sample (x = 0.0625). The tetragonal sample does not exhibit a loss in conductivity on thermal cycling, unlike the cubic sample, where the conductivity decreases due to a phase transformation from the cubic to the tetragonal phase. Variable temperature X-ray powder diffraction elucidated the structural transformations which the tetragonal bismuth niobate undergoes; from being tetragonal at room temperature, to cubic above 680 ^{o}C, then returning to the tetragonal phase upon cooling. To locate the interstitial oxygen atom positions in the tetragonal phase, powder neutron diffraction has been undertaken.

The magneto-structural transition in magnetocaloric $Mn_{1-x}Fe_xCoGe$

Q.Y. Ren[a], W.D. Hutchison[a], J.L. Wang[b], A.J. Studer[c], M.F. Md Din[b], S. Muñoz Pérez[a], J.M. Cadogan[a] and S.J. Campbell[a]

[a] *School of PEMS, The University of New South Wales, Canberra, ACT 2600, Australia.*

[b] *ISEM, University of Wollongong, Wollongong, NSW 2522, Australia.*

[c] *Bragg Institute, ANSTO, Lucas Heights, NSW 2234, Australia.*

Magnetic refrigeration techniques based on the magnetocaloric effect are considered an increasingly viable alternative to conventional gas-compression refrigerant, particularly with energy-saving and environmental aspects in mind. Following the discovery of a large magnetocaloric effect in $Gd_5Si_2Ge_2$ [1], researchers have shifted their attention to investigation of materials exhibiting magneto-structural transitions where large magnetic entropy changes are expected [2].

MnCoGe-based compounds are promising materials for the exploration of large magnetocaloric effects. They are relatively cheap (no rare earth elements) and, importantly, allow an appropriate temperature window (275 – 345 K) around room temperature in which the magneto-structural transition may be positioned. It has been established that Fe is a suitable substitute for Mn to 'tune' the structural transition temperature and hence obtain a magneto-structural transition [see e.g. 3, 4]. Here we present the results of a detailed investigation of the structural and magnetic properties and magnetocaloric effect for a range of as-prepared $Mn_{1-x}Fe_xCoGe$ alloys (x = 0.01, 0.02, 0.03 and 0.04) using temperature-variable x-ray diffraction (20 – 310 K), neutron diffraction (5 – 450 K) and physical properties measurement system (PPMS, 5 – 300 K). Particular attention will focus on analysis of neutron diffraction data for $Mn_{0.98}Fe_{0.02}CoGe$ and the nature of the magnetic phase-transition in $Mn_{0.98}Fe_{0.02}CoGe$.

[1] V.K. Pecharsky and K.A. Gschneidner Jr, *Phys. Rev. Lett.* **78**, 4494 (1997)

[2] E. Brück, *J. Phys. D: Appl. Phys.* **38**, R381 (2005).

[3] T. Samanta, I. Dubenko, A. Quetz, S. Stadler and N. Ali, *Appl. Phys. Lett.* **101**, 242405 (2012).

[4] Q.Y. Ren, W.D. Hutchison, J.L. Wang, S. Muñoz Pérez, J.M. Cadogan and S.J. Campbell, *Phys. Status Solidi (a)* **211**, 1101 (2014).

TN1

Dynamics of magnetic skyrmions: Theoretical design of skyrmion devices

W. Koshibae,[a] Y. Kaneko,[a] J. Iwasaki[b] and N. Nagaosa[a,b]

[a] *RIKEN Center for Emergent Matter Science (CEMS), Wako , Saitama 351-0198, Japan.*

[b] *Department of Applied Physics, The University of Tokyo, 7-3-1, Hongo, Bunkyo-ku, Tokyo 113-8656, Japan.*

The key to develop magnetic memory devices is nothing more than the control technique of the magnetic texture by external fields. Recent studies reveal that skyrmion, the swirling magnetic texture, is driven by a much smaller electric current density than that for the domain wall motion, and hence, the potential application of the skyrmion has attracted much attention. To utilise the skyrmion for device applications, the technique for creation (write), annihilation (eliminate) and motion (transport) must be established.

We theoretically study the creation, annihilation and current-driven motion of skyrmion in the chiral and dipolar magnets in two dimensions by numerically solving Landau-Lifshitz-Gilbert equation,

$$\frac{d\boldsymbol{n_r}}{dt} = \left(-\frac{\partial H}{\partial \boldsymbol{n_r}} \right) \times \boldsymbol{n_r} + \alpha \boldsymbol{n_r} \times \frac{d\boldsymbol{n_r}}{dt} \ , \tag{1}$$

where $\boldsymbol{n_r}$ is the normalised vector along magnetic moment, H is the Hamiltonian describing the magnetic system, and α denotes the Gilbert damping constant. By the numerical study, we explore the optimal condition to control the skyrmion in the ferromagnetic background.

The topology of the skyrmion is characterized by the skyrmion number,

$$N_{sk} = \frac{1}{4\pi} \int \boldsymbol{n_r} \cdot \left(\frac{\partial \boldsymbol{n_r}}{\partial x} \times \frac{\partial \boldsymbol{n_r}}{\partial y} \right) d^2 r, \tag{2}$$

which gives a wrapping number of a sphere by the magnetic moments. For the perfect ferromagnetic state $\boldsymbol{n_r}$=(0,0,+1), N_{sk}=0 and a skyrmion in the ferromagnetic background gives N_{sk}=−1. Because of the difference in topology, N_{sk}, the skyrmion cannot be reached from the perfect ferromagnetic state within the continuous deformation of the magnetic texture. As a result, the skyrmion carries a (meta-) stability and is protected by a potential barrier. To overcome the barrier, an energy being large enough to destroy the magnetic ordering is needed. However, the spatial discontinuity gives a favorable environment to change the topology of magnetic texture and the stability is reduced. For example, the skyrmion is created rather easily at the edge of a magnet in comparison to deep inside of the system. Also laser irradiation can induce a hot spot where the skyrmions are nucleated.

We show numerical results of the real-time dynamics in the magnetic textures induced by external stimuli and discuss the creation, annihilation and current-driven motion of skyrmion(s) for the theoretical design of the skyrmion memory devices.

Pressure-induced inter-site valence transitions involving geometric frustration in hexagonal perovskites

C.D. Ling[a], B.J. Kennedy[a] and M. Avdeev[b]

[a] *School of Chemistry, The University of Sydney, Sydney 2006, Australia.*

[b] *Bragg Institute, ANSTO, PMB 1, Menai 2234, Australia.*

Solid-state compounds are generally thought of as consisting of ions with well-defined oxidation states. While ionic bonds always have some degree of covalent character, the ionic approximation is usually sufficient to understand their "crystal chemistry" in conjunction with concepts such as bond valence sum (BVS) and effective ionic radius (IR). IR predicts that an atom will shrink as its oxidation state increases. This occurs gradually as electrons are removed within a shell (e.g., IR(Ir^{3+}) = 0.68, IR(Ir^{4+}) = 0.625, IR(Ir^{5+}) = 0.57 Å in 6-fold coordination), but removing the last electron of a shell produces a more pronounced change (e.g., IR(Bi^{3+}) = 1.03, IR(Bi^{5+}) = 0.76 Å). For a compound with a suitable combination of cations, it should therefore be possible to effect a net reduction in volume by transferring an electron from one to the other. A change in temperature and/or pressure could make such a valence state transition favourable; but in practice, such transitions are extremely rare.

We have observed such a pressure-induced charge transfer, from Bi to Ir (or Ru) in the hexagonal perovskites $Ba_{3+n}BiM_{2+n}O_{9+3n}$ (n = 0,1; M = Ir, Ru) [1,2] using high-pressure synchrotron x-ray and neutron powder diffraction. They all show ~1% first-order volume contractions at room temperature above 5 GPa, due to the large reduction in the IR of Bi when the 6s shell is emptied on oxidation. These are the first such transitions involving 4d and 5d compounds, and double the total number of cases ever observed. *Ab initio* calculations suggest that magnetic interactions through very short (~2.6 Å) *M*–*M* bonds contribute to the finely balanced nature of their electronic states.

[1] W. Miller, M. Avdeev, Q. Zhou, B.J. Kennedy, N. Sharma, R. Kutteh, G.J. Kearley, S. Schmid, K.S. Knight, P.E.R. Blanchard, C.D. Ling, *J. Am. Chem. Soc.* **134**, 3265-3270 (2012).

[2] Z. Huang, J.E. Auckett, P.E.R. Blanchard, B.J. Kennedy, W. Miiller, Q. Zhou, M. Avdeev, M.R. Johnson, M. Zbiri, G. Garbarino, W.G. Marshall, Q. Gu, C.D. Ling, *Angew. Chem. Int. Ed.* **53**, 3414-3417 (2014).

TN3

Violation of the Spin Statistics Theorem and the Bose-Einstein Condensation of Particles with Half Integer Spin

H.D. Scammell and O.P. Sushkov

School of Physics, University of New South Wales, NSW 2052, Australia.

We consider the Bose condensation of bosonic particles with spin 1/2. The condensation is driven by an external magnetic field. Our work is motivated by ideas of quantum critical deconfinement and bosonic spinons in spin liquid states. We show that both the nature of the novel Bose condensate and the excitation spectrum are fundamentally different from that in the usual integer spin case. We predict two massive ("Higgs") excitations and two massless Goldstone excitations. One of the Goldstone excitations has a linear excitation spectrum and another has quadratic spectrum. This implies that the Bose condensate does not support superfluidity, the Landau criterion is essentially violated. We formulate a "smoking gun" criterion for searches of the novel Bose condensation.

Yttria-stabilised zirconia: A trend study of structural, electronic and vibrational properties

G.P. Cousland[a,b], X.Y. Cui[c,d], A.E. Smith[e], A.P.J. Stampfl[b] and C.M. Stampfl[a,f]

[a] *School of Physics, The University of Sydney, NSW 2006, Australia.*

[b] *Bragg Institute, Australian Nuclear Science and Technology Organisation, Lucas Heights, NSW 2234, Australia.*

[c] *Australian Centre for Microscopy & Microanalysis, The University of Sydney, NSW 2006, Australia.*

[d] *School of Aerospace, Mechanical and Mechatronic Engineering, The University of Sydney, NSW 2006, Australia.*

[e] *School of Physics, Monash University, Victoria 3800, Australia.*

[f] *Department of Materials Science & Engineering, Yonsei University, Republic of Korea.*

Yttria-stabilised zirconia (YSZ) is an important ceramic, due to its dielectric properties and its strength, which is maintained at high temperature. Finding the structure of YSZ has proven difficult because it changes with temperature, yttria (Y_2O_3) concentration and sample preparation. Further, the scattering amplitudes of Zr and Y, for both x-rays and neutrons, are very similar and so cannot discriminate atom positions. Methods are used where state-of-the-art DFT code (DMol^3) simulations with 10.35 mol% Y_2O_3 are compared with x-ray photoemission spectroscopy to examine short-range order [1], and with inelastic neutron scattering to examine long-range order [2], for samples of YSZ with 8-9 mol%. Furthermore, YSZ with 10.35 mol% is used along with recently published models of 14, 17, 20 and 40 mol%, together with cubic, tetragonal and monoclinic zirconia (ZrO_2), in a trend study which shows an increase in band-gap (0.73 eV) and decrease in valence band (2.0 eV) across the range of increasing Y_2O_3 concentration and relative to cubic ZrO_2 [3].

[1] G.P. Cousland, X.Y. Cui, A.E. Smith, C.M. Stampfl, L. Wong, M. Tayebjee, D. Yu, G. Triani, P.J. Evans, H.-J. Ruppender, L.-Y. Jang and A.P.J. Stampfl, *J. Appl. Phys.* **115**, 143502 (2014).

[2] G.P. Cousland, R.A. Mole, M.M. Elcombe, X.Y. Cui, A.E. Smith, C.M. Stampfl and A.P. J. Stampfl, *J. Phys. Chem. Solids* **75**, 351 (2014).

[3] G.P. Cousland, X.Y. Cui, S. Ringer, A.E. Smith, A.P.J. Stampfl and C.M. Stampfl, *J. Phys. Chem. Solids* **75**, 1252 (2014).

TN5

Electron-Phonon Coupling in Epitaxial Silicene: Scanning Tunneling Microscopy and Raman Studies

Y. Du, J.C. Zhuang, X. Xu and S.X. Dou

Institute for Superconducting and Electronic Materials, University of Wollongong, Wollongong, NSW 2500 Australia.

Silicene, which is single layer of silicon atoms packed in a honeycomb structure, has attracted enormous interest due to its Dirac fermion characteristics and a wide range of promising applications. Epitaxial silicene demonstrates a strong interaction with the substrate that dramatically affects its electronic structure. We report that the special coupling between Dirac fermion and lattice vibrations, in other words, electron-phonon coupling (EPC), in silicene layers on Ag(111) surface was probed by *in-situ* Raman spectroscopy. We find the EPC is significantly modulated due to tensile strain, which results from the lattice mismatch between silicene and the substrate, and the charge doping from the substrate. The special phonon modes corresponding to two-dimensional electron gas scattering at edge sites in the silicene were identified. Detecting relationship between EPC and Dirac fermion through the Raman scattering will provide a direct route to investigate the exotic property in buckled two-dimensional honeycomb materials.

TA1

Domain walls and phase boundaries - new nanoscale functional elements in complex oxides

J. Seidel

School of Materials Science and Engineering, UNSW Australia, NSW 2032, Australia.

email: jan.seidel@unsw.edu.au, http://www.materials.unsw.edu.au/profile/jan-seidel

Interfaces and topological boundaries in complex oxide materials, such as domain walls and morphotropic phase boundaries, have recently received increasing attention due to the fact that their properties, which are linked to the inherent order parameters of the material, its structure and symmetry, can be completely different from that of the bulk material [1]. I will present an overview of recent results on electronic and optical properties of ferroelectric phase boundaries, domain walls, and topological defects in multiferroic materials [2, 3, 4, 5, 6]. The origin and nature of the observed confined nanoscale properties is probed using a combination of nanoscale transport measurements based on scanning probe methods, high resolution transmission electron microscopy and first-principles density functional computations. I will also give an outlook on how these special properties can be found in other material systems and discuss possible future applications [7].

[1] J. Seidel, et al., *Nature Materials* **8**, 229 (2009).

[2] J. Seidel, et al., *J. Phys. Chem. Lett.* **3**, 2905 (2012).

[3] J. Seidel, et al., *Phase Trans.* **86**, 53 (2013).

[4] J. Seidel, et al., *Adv. Mater.* **26**, 4376 (2014).

[5] Y. Heo, et al., *Adv. Mater.*, DOI: 10.1002/adma.201401958 (2014).

[6] K.-E. Kim, *NPG Asia Mater.* **6**, e81 (2014).

[7] G. Catalan, J. Seidel, R. Ramesh, and J. Scott, *Rev. Mod. Phys.* **84**, 119 (2012).

TA2

Cobalt-palladium multilayer films for hydrogen gas sensing

C. Lueng, Peter J. Metaxas and M. Kostylev

School of Physics, University of Western Australia, Crawley 6009, Australia.

Recently it has been found that hydrogen gas (H_2) absorption by a Pd capping layer results in a shifted ferromagnetic resonance (FMR) of the underlying ferromagnetic layer. This effect was explained as originating from variation in the magnetic anisotropy of the cobalt layer [1], opening a route for the development of magnetic and spintronic Hydrogen gas sensors. In this work, we have measured the FMR response of a number of cobalt-palladium (Co/Pd) based multilayer thin films under hydrogen charging at atmospheric pressure in order to identify the dependency of the H_2-modified FMR response to the film composition, results which are important for optimising these materials for H_2 sensing.

Specifically, we will discuss the dependency of the shift of the resonance peak on the Co layer thickness, *t*, for two multilayer thin film structures: a bilayer //Co/Pd film and a trilayer //Pd/Co/Pd film, both grown on Silicon substrates via dc magnetron sputtering in argon atmosphere. A custom made air-tight cell was manufactured to enable controlled continuous flow of gas at atmospheric pressure through the chamber while performing FMR experiments. The cell contains a coplanar waveguide on which the film sits which is connected to a microwave generator and receiver to measure the films' FMR absorption signals at a fixed microwave frequency under a swept magnetic field, *H*, applied in the sample plane. For the bi-layer films we find that the H_2-induced shift of the FMR field, decreases with an increase in the Cobalt layer thickness. This confirms the interfacial nature of the effect, which is consistent with the existence of an interfacial, perpendicular magnetic anisotropy at the Pd-Co interface. The thickness dependence of the shifts observed for the tri-layer structures however is non-monotonic, meriting further study.

Financial support by the Australia Research Council and an Australian Postgraduate Award is acknowledged.

[1] C.S. Chang, M. Kostylev and E. Ivanov, *Appl. Phys. Lett.* **102**, 142405 (2013).

TA3

Polarised Neutrons for Materials Research on OPAL Instruments

W.T. Lee

Bragg Institute, Australian Nuclear Science and Technology Organisation, New South Wales 2234, Australia.

Polarised neutron scattering is a powerful technique to study magnetism and to enhance the signal-to-noise in the studies of hydrogen-rich materials in biology and organic chemistry. Polarisation analysis unambiguously identifies the scattering pattern of the magnetic structure and excitation and determines the direction of magnetic moment and excitation. Using polarisation analysis in neutron scattering to measure hydrogen-rich materials, we can separately measure the structural signal and the amount of hydrogen in the material, which has long been a challenge in studying organic materials. At ANSTO, polarisation analysis has previously been available on the reflectometer PLATYPUS for thin film and multilayer studies. The operation of a ^{3}He Polarising Station has now provide this capability to the WOMBAT diffractometer for determining magnetic structure down to the atomic level and to the TAIPAN triple-axis spectrometer for studying magnetic excitation and structure. During commissioning tests, we have discovered new details of magnetic structure in multiferroic samples on both instruments. This new development will soon be followed by polarised SANS capability on QUOKKA for magnetic nano-particle and hydrogen-rich material research. Off-specular magnetic scattering on reflectometer PLATYPUS and polarised inelastic scattering on spectrometers PELICAN and SIKA will be made available in the coming months.

TA4

^{57}Fe Mössbauer Study of the Chainpur meteorite

N. N. Elewa, R. Cobas, W. D. Hutchison and J. M. Cadogan

School of Physical, Environmental and Mathematical Sciences, The University of New South Wales at the Australian Defence Force Academy, Canberra 2610, Australia.

The Chainpur meteorite is one of 23 meteorites that are classified as an ordinary chondrite of the petrologic group LL3. It fell as a shower of stones on May 9, 1907 in Uttar Pradesh, India (25° 51' N / 83° 29' E) [1] . We report here the characterisation of the Fe-bearing phases in this chondrite using ^{57}Fe Mössbauer spectroscopy carried out at 298 K, 100 K, 50 K and 13 K. The paramagnetic doublets of olivine and pyroxene dominate the room temperature spectrum, accounting for around 70% of the spectral area. There are also magnetically split components corresponding to troilite and iron-nickel metal (kamacite). On the basis of the measured ^{57}Fe electric quadrupole splitting we estimate the mean Fe:Mg ratio in this meteoritic olivine to be around 35:65 % although there is clearly a wide range of composition [2].

[1] M. M. Grady, *Catalogue of Meteorites*, 5th ed (Cambridge University Press, 2000) p 689.

[2] O. N. Menzies, P. A. Bland and F. J. Berry, *Lunar Planet. Sci. XXXII*, pp. 1967–1968, (2001).

TA5

Neutron scattering's influence on crystallography

G.J. McIntyre

Australian Nuclear Science and Technology Organisation, Lucas Heights NSW 2234, Australia.

Picture a group of X-ray diffractionists pontificating in the Crystallography Forum; the buffoon amongst them asks: "What has neutron diffraction done for us?"

Aside from being a poor parody of a well-known scene from a Monty Python film, this question does contain an element of truth. In the hundred years since the discoveries of von Laue and the Braggs, X-ray crystallography has been remarkably successful in providing extensive and reliable tools and methods for understanding many aspects of crystal structure and behavior. There are, of course, particular experiments where neutrons offer significant advantages over X-rays. These advantages are well known to us all: dramatically different dependence of the scattering factors on atomic number and isotope, no dependence of the nuclear scattering factor on angle, larger penetration, sensitive to unpaired spins, and energies comparable to lattice and magnetic excitations. But what has neutron scattering contributed to the science of crystallography?

With the ringing out of 2014 as the UNESCO International Year of Crystallography, it is timely to reflect on the various aspects of crystallography where neutrons have led the way [1]. These aspects include the development of counter diffractometers, automation, and electronic position-sensitive detectors, most areas of magnetism, the study of incommensurate structures, the Rietveld method to analyse powder diffraction patterns, total pattern refinement, powder diffraction in materials discovery, standard libraries of amino acids and peptides, strain scanning, extreme sample environments of many forms, and *operando in situ* experiments.

Potted histories of several of these aspects, especially those with connection to the neutron scattering activities at Lucas Heights, will be presented.

[1] G.J. McIntyre, *Neutron News.* **25**, 15 (2014).

TP1

EMU, the cold-neutron backscattering spectrometer at the Bragg Institute, ANSTO

N. de Souza, A. Klapproth and G.N. Iles

Australian Nuclear Science and Technology Organisation, The Bragg Institute, Lucas Heights NSW, Australia.

The Bragg Institute is currently in the final installation stage of a cold-neutron backscattering spectrometer in the ANSTO OPAL research reactor neutron guide hall. This spectrometer, called EMU, is based on Si (111) crystal backscattering and extracts neutrons from a cold neutron guide via a double HOPG (002) crystal premonochromator setup. Backscattering occurs through implementation of spherical focusing between the Si (111) crystal monochromator and analyser arrays, aiming to deliver a spectrometer FWHM energy resolution in the order of 1.2 μeV. EMU also features a 7-metre long focusing guide located between the two premonochromators, a so-called graphite chopper alternating beam delivery to the backscattering crystal monochromator and then into the secondary spectrometer [1], and a linear Doppler drive modulating incident neutron energies over ± 31 μeV. Scattered, analysed neutrons are counted in ^{3}He LPSD arrays.

EMU is provisioned for future extensions of its dynamic range via higher-resolution, undeformed Si (111) crystal analyser arrays, and variable HOPG (002) crystal premonochromator reflection angles.

Access to the EMU spectrometer will be via beam-time requests to the OPAL neutron-beam user facility. EMU is ideally suited for measuring relaxation times from a few 10 ps to over 1 ns, for momentum transfers up to 2 Å^{-1}, and readily from cryogenic temperatures up to 700 K.

[1] B. Frick and M. Gonzalez, *Physica B* **301**, 8 (2001).

Mössbauer observation of the Mobility of Cl^- Ions in a Frozen Solution

J.D. Cashion[a], T.K. Choo[b] and L. Zhang[b]

[a] *School of Physics, Monash University, Victoria 3800, Australia.*

[b] *Department of Chemical Engineering, Monash University, Victoria 3800, Australia.*

When a liquid is frozen, the crystallographic arrangement of the frozen material depends on the speed of freezing. However, with aqueous solutions, we usually consider that, once frozen, they then remain unchanged unless allowed to come up to near 0° C. However, we have observed the effect of the migration of Cl^- ions at -80º C. The samples were from a series of coal combustion products and in the course of evaluating the iron coordination and valence of the combustion products and their eluents, we took ^{57}Fe Mössbauer spectra of frozen solutions of iron-containing eluents in 2M HCl.

The samples for Mössbauer spectroscopy were prepared by encapsulating approximately 1 ml of the solution in a Perspex piston type capsule while leaving a small air gap to allow for the expansion of the liquid, sealing it with Perspex dissolved in dichloromethane and then placing it into a small dewar of liquid nitrogen to rapidly freeze it. Since the only reason for freezing the sample was to enable a Mössbauer spectrum to be obtained, 77 K was colder than required. It was expected that the runs would take approximately one week each, so it was decided, for economy reasons, to use dry ice to provide a constant 193 K temperature environment. Spectra were taken over a period of five days for one sample and ten days for the second, but saved in a daily basis.

The spectra consisted of two ferrous doublets and one ferric doublet. However, the surprising feature was that the relative intensities of the two ferrous doublets changed with time during the run. The outer doublet (IS = 1.27 mm/s, QS = 3.16 mm/s) is due to Fe^{2+} ions coordinated to an octahedron of water molecules, $[Fe(H_2O)_6]^{2+}$ [1] and this increased steadily in intensity. The inner doublet (IS = 1.34 mm/s, QS = 1.62 mm/s) is a glassy phase with Cl^- ions being incorporated in the inner coordination sphere. The ratio of the two sites changed from 0.26:1 to 1.7:1 over 5 days as the sample crystallised.

[1] A. Vertes and D.L. Nagy, *Mössbauer Spectroscopy of Frozen* Solutions, (Akad. Kaido, Budapest, 1990) p 61.

TP3

Cusp Singularities and Magnetisation Plateaux in a Frustrated Spin Ladder

T. Sugimoto[a], M. Mori[b], T. Tohyama[a], and S. Maekawa[b]

[a] *Faculty of Science, Tokyo University of Science, Katsushika, Tokyo, Japan.*

[b] *Advanced Science Research Center, Japan Atomic Energy Agency, Tokai, Ibaraki, Japan.*

Recently, a cascade of phase transitions induced by magnetic field has been observed in $BiCu_2PO_6$ [1,2], whose effective spin model, a frustrated two-leg spin ladder, bridges between the frustrated spin chain and the non-frustrated spin ladder with one-half spins [2,3]. According to the theoretical studies, the zigzag spin chain exhibits one-third plateau [4], although no plateau emerges in the non-frustrated spin ladder [5]. Therefore, the simple question arises as to whether plateaux do appear in the frustrated spin ladder, or not. To clarify the question, we calculate rung-coupling dependence and frustration dependence of magnetisation process by using density-matrix renormalisation-group method. In this calculation, we find some plateaux at m=1/2 and 2/3, which do not appear in both the frustrated spin chain and the non-frustrated spin ladder, in addition to 1/3 plateau and some cusps [6]. We analytically find out a correspondence between effective models in weak and strong rung-coupling limits, which gives an explanation of the plateaux and cusps.
Our study is useful to analyze experimental data of $BiCu_2PO_6$.

[1] Y. Kohama, S. Wang, A. Uchida, K. Prsa, S. Zvyagin, Y. Skourski, R. D. McDonald, L. Balicas, H.M. Ronnow, C. Rüegg and M. Jaime, *Phys. Rev. Lett.* **109**, 167204 (2012).

[2] A.A. Tsirlin, I. Rousochatzakis, D. Kasinathan, O. Janson, R. Nath, F. Weickert, C. Geibel, A.M. Lauchli and H. Rosner, *Phys. Rev. B* **82**, 144426 (2010).

[3] T. Sugimoto, M. Mori, T. Tohyama and S. Maekawa, *Phys. Rev. B* **87**, 155143 (2013).

[4] K. Okunishi and T. Tonegawa, *J. Phys. Soc. Jpn.* **72**, 479 (2003); *Phys. Rev. B* **68**, 224422 (2003).

[5] D. Cabra, A. Honecker and P. Pujol, *Phys. Rev. Lett.* **79**, 5126 (1997).

[6] T. Sugimoto, M. Mori, T. Tohyama and S. Maekawa, *arXiv:*1409.4280.

TP4

The square lattice quantum ANNNH model revisited: Does the model support a '2+2' phase?

J. Oitmaa[a] and R.R.P Singh[b]

[a] *School of Physics, University of New South Wales, Sydney N.S.W. 2052, Australia.*

[b] *Department of Physics, University of California, Davis, CA 95616, U.S.A.*

Recent studies of intercalated FeSe materials [1,2] have indicated a novel type of magnetic order at low temperatures. Inelastic neutron scattering shows the strongest magnetic peak near (π, $\pi/2$), indicative of a 2 x 4 magnetic unit cell. Electronic structure calculations [2] support a '2+2' state, with 2 up spins followed by 2 down spins, in columns, with adjacent columns coupled antiferromagnetically.

A possible Heisenberg model which might show such a phase is the 'ANNNH' (axial next-nearest-neighbour Heisenberg) model. This is a generalisation, to vector spins, of the much studied Ising version (ANNNI model) which has been shown to support such a 2+2 phase. Classically, the ANNNH model shows a transition from a Néel phase to an incommensurate spiral at the point $J_2/J_1 = 0.25$. However, for quantum spins, and particularly for the extreme quantum case S = ½, the phase diagram is not known.

This work studies the phase diagram of the ANNNH model, to see if such a 2+2 phase is supported in some range of the parameters. We use series expansion methods [3], both at T = 0 and at high T, to explore this possibility. The result is largely negative, in the sense that a 2+2 phase is not energetically favoured. However, the Néel-spiral transition is found to occur at $J_2/J_1 \sim 0.45$, considerably higher than the classical value.

[1] A.E. Taylor, S.J. Sedlmaier, S.J. Cassidy, E.A. Goremychkin, R.A. Ewings, T.G. Perring, S.J. Clarke and A.T. Boothroyd, *Phys. Rev. B* **87**, 220508(R) (2013).

[2] H.-Y. Cao, S. Chen, H. Xiang, X.-G. Gong, *arXiv:* 1407.7145 (2014).

[3] J. Oitmaa, C.J. Hamer and W.-H. Zheng, *Series Expansion Methods for Strongly Interacting Lattice Models* (Cambridge University Press Press, 2006).

TP5

Terahertz emission by ultrafast cathode erosion processes in electrical discharge

J. Horvat, E. Constable and R.A. Lewis

School of Physics and ISEM, University of Wollongong, New South Wales 2522, Australia.

Unwinding sticky tape was shown to result in weak non-thermal terahertz radiation [1], however the mechanism is unclear. A candidate mechanism for this radiation is electric discharge through air, as breaking of chemical bonds upon the unwinding creates a local electric field on the tape. To test the plausibility of this mechanism, we study the radiation produced in electrical discharge between two electrodes in air, at atmospheric pressure.

Our electrodes consisted of a pointed stainless steel anode and a flat Fe cathode. The distance between the electrodes was adjusted with a micrometer. A capacitor was charged up to 1300 V and discharged through the air gap between the electrodes. The resulting radiation was first filtered, passing only the radiation between 3 and 9 THz on to a helium-cooled Si bolometer detector. The output voltage of the bolometer was recorded by a fast digital oscilloscope.

For large distances between electrodes (> 20 μm) and low capacitor voltage (< 1000 V), only thermal radiation was observed in the bolometer output voltage. However, several sharp voltage spikes were observed on top of the thermal background with an electrode gap of 5 μm and capacitor voltage 1300 V. Considering that the bolometer is filtered to measure only in the 3-9 THz frequency range, the processes producing this radiation have to occur at time-scales of ~ 0.1 ps. We explain this through the melting of cathode micro-protrusions as large current densities pass through them [2]. The melting results in micro-explosions and a sudden release of electrons into the electrode gap, producing large currents on short time-scales [2].

Because we detected only thermal terahertz radiation for small electrical fields through the electrode gap, for which the cathode micro-explosions do not occur, we conclude that electrical discharge is unlikely mechanism of terahertz radiation by unwinding adhesive tape.

[1] J. Horvat and R.A. Lewis, *Optics Letters* **34**, 2195 (2009).

[2] G.A. Mesyats, *Plasma Phys. Control. Fusion,* **47**, A109 (2005).

TP6

Confinement due to spin-orbit interaction in quantum point contacts

Tommy Li

School of Physics, University of New South Wales, Australia.

One-dimensional systems with spin-orbit interaction have been hotly studied in recent years as both candidates for injectors and detectors of spin current [1], and for their role in the search for emergent Majorana fermions [2]. I describe the properties of a quantum point contact (QPC) in the presence of the spin-orbit interaction and external magnetic field using scattering theory. It is shown that Dirac fermion states appear leading to confinement of particles in the constriction and resonances in the QPC conductance. The spacing of resonances can be tuned by the external magnetic field. Experimentally, the level spacing can be made narrow, transforming the QPC into a deep trap. This effect is directly analogous to surface and edge states in three- and two-dimensional topological insulators, and represents a manifestation of emergent Dirac physics in a one-dimensional channel.

[1] F. Mireles and G. Kirczenow, *Phys. Rev. B* **64**, 024426 (2001).

[2] R.M. Lutchyn, J.D. Sau, and S. Das Sarma, *Phys. Rev. Lett.* **105**, 077001 (2010).

TP7

Strong Spin-Orbit Coupling Effects Driven by an External Magnetic Field and the Anisotropic Zeeman Effect in 2D GaAs (InAs) Quantum Dots

D.S. Miserev and O.P. Sushkov

School of Physics, University of New South Wales, NSW 2033, Australia.

Spin-orbit interaction effects dramatically affect the band structure of zink-blende semiconductors such as GaAs or InAs separating spin-1/2 and spin-3/2 valence bands with the spin-orbit gap of order of hundreds of meV. This splitting acknowledges to forget about the spin-1/2 band and the hole spectrum in the vicinity of the Γ-point (the top of the spin-3/2 band) is described by the Kohn-Luttinger Hamiltonian.

Consider next the 2D semiconductor film, width *d*, with the frozen quasi-momentum π / d along z-axis. The spin-orbit coupling term in the Kohn-Luttinger Hamiltonian leads to the gap between projections $\pm 3/2$ (heavy holes) and $\pm 1/2$ (light holes) being open. For the typical width of 20 nm the gap reaches the value of 10 meV meanwhile the energy of the in-plane motion is about of 1 meV which provides the opportunity to consider such a 2D systems via the perturbative approach.

Current study concerns the influence of the in-plane magnetic field on electronic properties of 2D hole quantum dots. Slight mixing between split heavy hole and light hole bands leads to effective spin-orbit corrections to the spectrum of heavy holes which arise from the ordinary Zeeman term entangling projections 1/2 and 3/2 (-1/2 and -3/2). As we have shown, such a spin-orbit interaction does not lift completely the degeneracy of energy levels for circle quantum dots: some of levels remain two-fold degenerate. Moreover, level-crossings with the change of degeneracy have been predicted at sufficiently large magnetic fields of order of 10 T. The residual degeneracy can be lifted by B^3 corrections and the dot's ellipticity.

Further, we consider anisotropic contributions g_{xz} to g-factor which come from the tensor part of the Kohn-Luttinger Hamiltonian. The urgency of this problem appeared as the result of the sign discrepancy between recent theoretical predictions and the experimental data. As the result, we provided contributions which are responsible for the change of the g_{xz} sign.

TP8

Electron tunneling across potential barrier in AA-stacked graphene

M. Sanderson, Y. S. Ang and C. Zhang

School of Physics, University of Wollongong, Wollongong, NSW 2500, Australia.

The tunneling probability of electrons across n-p and n-p-n junctions has been calculated and Klein tunneling has been found to occur. Klein tunneling is the phenomenon whereby electrons can be perfectly transmitted across a junction even though a potential difference may exist.

Tunneling across this junction is also found to conserve the 'cone index' of the electron, which relates to the band structure of AA-stacked graphene.

Due to this conservation requirement electrons can be separated due to their cone index. Fabry-Pérot resonances are seen to occur in the n-p-n system, which allows for perfect transmission at oblique incident angles. The conductance across a barrier is also calculated.

Enhancement of magnon mediated coupling between fermions in a vicinity of a magnetic quantum critical point

Y. Kharkov and O. Sushkov

School of Physics, University of New South Wales, NSW 2052, Australia.

Superconducting pairing in cuprates is widely believed to be driven by a magnetic mechanism. Recent experiments [1,2] with underdoped cuprates, meanwhile, proved the existence of a magnetic quantum critical point (QCP), separating phases with no static magnetic order and with magnetic order. The QCP for $YBa_2Cu_3O_y$ is located at a doping of $x \approx 0.1$ [1-3], which is quite close to the optimal doping of $x \approx 0.15$, where maximum of $T_c(x)$ reaches. The idea is that superconducting pairing can be significantly influenced by magnetic criticality, which has been recently considered by Wang, and Chubukov [4] in the context of electron doped cuprates. A common approach to such problems is to treat electrons in the normal state as a Fermi liquid with a large Fermi surface, implying a weak coupling regime. However, a large Fermi surface, to a significant extent, diminishes the importance of the magnetic criticality. In the present work, we consider a "rigid" 2D Mott insulator with two immobile fermions injected, so in essence our approach implies a small Fermi surface and therefore strong coupling limit. As a model system we consider a 2D bilayer antiferromagnet that is close to the $O(3)$ magnetic quantum critical point (QCP), separating magnetically ordered and disordered phases. Focusing on the disordered phase in the vicinity of the QCP, we demonstrate that the criticality results in a strong long range attraction between the fermions, with a potential $V(r) \propto 1/r^{0.75}$, where r is the separation between the fermions. The mechanism of the enhanced attraction is similar to the Casimir effect and it is also closely related to the spin-charge separation at the QCP. So we suggest a mechanism of magnetic critical enhancement of pairing in cuprates.

[1] C. Stock, W.J.L. Buyers, Z. Yamani, Z. Tun, R.J. Birgeneau, R. Liang, D. Bonn and W. N. Hardy, *Phys. Rev. B* **77**, 104513 (2008).

[2] D. Haug, *New J. Phys.* **12**, 105006 (2010).

[3] A.I. Milstein and O.P. Sushkov, *Phys. Rev. B* **78**, 014501 (2008).

[4] Y. Wang and A.V. Chubukov, *Phys. Rev. B* **88**, 024516 (2013).

TP10

The Capacitive Current and Conduction Current of Zinc Oxide Varistor Ceramic Materials for Nanosecond Pulse Electronic Breakdown

G. Xie[a,b] and W. Shi[a]

[a] *The Department of Applied Physics, Xi'an University of Technology. Xi'an 710048, China.*

[b] *The School of Physics, University of Wollongong. NSW 2500, Australia.*

ZnO varistors are employed to protect for the electric circuits of information system, control system and high voltage engineering. Many studies on the pulse response of ZnO varistors used pulse power supplies or spark-gap more pulse power to provide electrical pulse excitation. The test system is designed to study the pulse response of ZnO varistor ceramics at DC bias.[1] Both capacitive current i_C and conduction current i_R is clearly observed in the ultrafast electric current pulse output by ZnO varistors.

The test results can be analyzed by using the switching characteristics of PCSS's and the conduction mechanisms of ZnO varistor ceramics. In the linear mode of SI-GaAs PCSS's, the composite electric pulse with capacitance current i_C and conduction current i_R can be obtained when the ZnO grain boundary is broken down. Because it needs to take some time to break down ZnO grain boundaries[2], and then, the capacity of grain boundaries decays rapid and the varistors sends out a conductance current, there is a certain delay between i_R and i_C which is observed clearly. These ultrafast pulse response characteristics of ZnO varistor ceramics provide an experimental data for the rationality of the theory of ZnO grain boundary.

Acknowledgments: This work was supported by the National Natural Science Foundations of China under grant 50837005 and the Nature Research Foundation of Xi'an University of Technology under grant no.2014TS017.

[1] W. Shi and G. Xie. *J. Am. Ceram. Soc.* **96**, 2179 (2013).

[2] G.D. Mahan, L.M. Levinson and H.R. Philipp. *J. Appl. Phys.* **50**, 2799 (1979).

TP11

Effects of Coulomb screening and disorder on artificial graphene based on nanopatterned semiconductor

O.A. Tkachenko[a], V.A. Tkachenko[a,b], I.S. Terekhov[c] and O.P. Sushkov[c]

[a] *Rzhanov Institute of Semiconductor Physics of SB RAS, Novosibirsk, 630090,Russia.*

[b] *Novosibirsk State University, Novosibirsk, 630090, Russia.*

[c] *School of Physics, University of New South Wales, NSW 2052, Australia.*

A residual disorder in the gate system is the main problem on the way to create artificial graphene based on two-dimensional electron gas. The disorder can be significantly screened/reduced due to the many-body effects. To analyse the screening/disorder problem we consider AlGaAs/GaAs/AlGaAs heterostructure with two metallic gates. We demonstrate that the design least susceptible to the disorder corresponds to the weak coupling regime (opposite to tight binding) which is realised via system of quantum anti-dots. The most relevant type of disorder is the area disorder which is a random variation of areas of quantum anti-dots. The area disorder results in formation of puddles. Other types of disorder, the position disorder and the shape disorder, are practically irrelevant. The formation/importance of puddles dramatically depends on parameters of the nanopatterned heterostructure. A variation of the parameters by 20-30% can change the relative amplitude of puddles by orders of magnitude. Based on this analysis we formulate criteria for the acceptable design of the heterostructure aimed at creation of the artificial graphene.

TP12

Evolution of magnetic phase and cation distribution in $Cu_{1-x}Zn_xFe_2O_4$ studied by neutron powder diffraction

F.F. Chang[a], G.C. Deng[b], M. Avdeev[b], J. Bertinshaw[a,b], J. Hester[b] and C. Ulrich[a,b]

[a] *School of Physics, University of New South Wales, Kensington, 2052 NSW, Australia.*

[b] *The Bragg Institute, Australian Nuclear Science and Technology Organisation, Lucas Heights, Australia.*

$CuFe_2O_4$ is a highly interesting material as it is a ferrimagnet with an unusual high magnetic ordering temperature of 780 K. $ZnFe_2O_4$, on the other hand, is a frustrated spin system with antiferromagnetic order below 10 K. By doping nonmagnetic Zn ions in $CuFe_2O_4$, frustration can be introduced and interesting properties might emerge. Given that, high resolution and high intensity neuron powder diffraction techniques have been applied to study the structural and magnetic phase transition in $Cu_{1-x}Zn_xFe_2O_4$ from 4 K to 750 K. Coexistence of cubic and tetragonal structure in $CuFe_2O_4$ was observed in a wide temperature range, which indicates a second order phase transition nature. This transition is caused by Jahn-Teller distortion of the CuO_6 octahedra. Although $CuFe_2O_4$ and $ZnFe_2O_4$ are inverse and normal spinels, respectively, mixed cation distribution was found in doped samples, with Cu and Zn ions sitting both either on the tetrahedral or the octahedral sites. All the doped $Cu_{1-x}Zn_xFe_2O_4$ (x = 0.2 - 1) samples crystallise in the cubic structure and order in the ferrimagnetic spin configuration. Upon doping, the value of oxygen position parameter μ increases, indicating the compression of the octahedra with increasing Zn-composition.

Short-range antiferromagnetic order was observed below 10 K in cubic $ZnFe_2O_4$. The spin frustration, which leads to the antiferromagnetic order in $Cu_{0.04}Zn_{0.96}Fe_2O_4$ and $ZnFe_2O_4$ is induced by the competing interaction between the first nearest neighbor and the third nearest neighbour tetrahedra formed by Fe ions on B sites [1,2].

[1] S. Soliman, A. Elfalaky, G.H. Fecher and C. Felser, *Phys. Rev. B* **83**, 085205 (2011).

[2] K. Kamazawa, Y. Tsunoda, H. Kadowaki and K. Kohn, *Phys. Rev. B* **68**, 024412 (2003).

TP13

Enhancement of T_C in Fe-based superconducting films by strain effect

J.C. Zhuang[a,b], Y. Du[a], X. Xu[a] and S. X. Dou[a]

[a] *Institute for Superconducting and Electronic Materials, University of Wollongong, Wollongong, NSW 2500 Australia.*

[b] *Department of Physics, Southeast University, Nanjing 210018, China.*

The effects of iron deficiency in FexSe0.5Te0.5 thin films (0.8<x<1) on superconductivity and electronic properties have been studied. A significant enhancement of the superconducting transition temperature (TC) up to 21K was observed in the most Fe deficient film (x=0.8). Based on the observed and simulated structural variation results, there is a high possibility that Fe vacancies can be formed in the FexSe0.5Te0.5 films. The enhancement of TC shows a strong relationship with the lattice strain effect induced by Fe vacancies. Importantly, the presence of Fe vacancies alters the charge carrier population by introducing electron charge carriers, with the Fe deficient film showing more metallic behavior than the defect-free film. Our study provides a means to enhance the superconductivity and tune the charge carriers via Fe vacancy, with no reliance on chemical doping.

TP14

The magnetic properties and magnetocaloric effect in $Mn_{1-x}Ni_xCoGe$

Q.Y. Ren[a], W.D. Hutchison[a], J.L. Wang[b], A.J. Studer[c] and S.J. Campbell[a]

[a] *School of PEMS, The University of New South Wales, Canberra, ACT 2600, Australia.*

[b] *ISEM, University of Wollongong, Wollongong, NSW 2522, Australia.*

[c] *Bragg Institute, ANSTO, Lucas Heights, NSW 2234, Australia.*

MnCoGe-based compounds reveal promise for magnetic refrigeration and as such have been extensively investigated over the last decade [1]. Refrigeration based on magnetic cooling *via* the magnetocaloric effect offers potential as an alternative to conventional gas-compression systems. MoCoGe-based compounds have two crystallographic structures: nominally low temperature TiNiSi-type orthorhombic structure (P*nma*) and the high temperature Ni_2In-type hexagonal structure (P$6_3/mmc$). When the structural transition temperature between these two structures is 'tuned' between the respective Curie temperatures of the phases (~345 K for the orthorhombic phase and ~275 K for the hexagonal phase [1]), a magneto-structural transition can be obtained. Such a transition allows a direct change from the ferromagnetic orthorhombic phase to the paramagnetic hexagonal phase [1]. For a magneto-structural transition, the lattice and magnetic entropy changes occur simultaneously, thereby providing scope for observation of a large magnetocaloric effect [2].

The crystallographic structures and magnetic properties of annealed $Mn_{1-x}Ni_xCoGe$ (x = 0.02, 0.03, 0.04, 0.05, 0.06 and 0.07) have been investigated using variable temperature X-ray diffraction and neutron diffraction (T = 5 - 320 K) with neutron diffraction measurements carried out both with and without applied magnetic fields for $Mn_{0.95}Ni_{0.05}CoGe$ (B = 0 - 8 T). Such experiments allow separation of the structural and magnetic contributions to the total entropy change at a magneto-structural transition [3]. The magnetic entropy changes have been derived in the conventional way from a series of isothermal magnetisation experiments, e.g. $-\Delta S_m$ ~8.8 J kg^{-1} K^{-1} for a magnetic field change of ΔB = 0 - 5 T in $Mn_{0.95}Ni_{0.05}CoGe$.

[1] N.T. Trung, L. Zhang, L. Caron, K.H.J. Buschow and E. Brück, *Appl. Phys. Lett.* **96**, 172504 (2010).

[2] J. Liu, T. Gottschall, K.P. Skokov, J.D. Moore and O. Gutfleisch, *Nat. Mater.* **11**, 620 (2012).

[3] J.L. Wang, L. Caron, S.J. Campbell, S.J. Kennedy, M. Hofmann, Z.X. Cheng, M.F. Md Din, A.J. Studer, E. Brück and S.X. Dou, *Phys. Rev. Lett.* **110**, 217211 (2013).

3D Printed Terahertz Diffraction Gratings and Lenses

A.D. Squires, E. Constable and R.A. Lewis

Institute for Superconducting and Electronic Materials, and School of Physics, University of Wollongong, NSW 2522, Australia..

3D printing opens up an inexpensive, rapid and versatile path to the fabrication of optical elements suited to the terahertz regime. The transmission of the plastics used in 3D printers, while generally decreasing with frequency, is usable over the range 0.1–2 THz. We have designed [1], fabricated, and tested regular and blazed gratings (Fig.1) and aspherical lenses [2] for operation at terahertz frequencies. We find that the measured performance matches our theoretical predictions. Characterisation of varying types of commercial 3D printer plastics has been performed. These include: Polylactic acid (PLA), Acrylonitrile Butadiene Styrene (ABS), Visijet crystal and an acrylic based polymer. Data was taken using a 2 colour wave photomixing system and at the Australian Centre for Synchrotron Science.

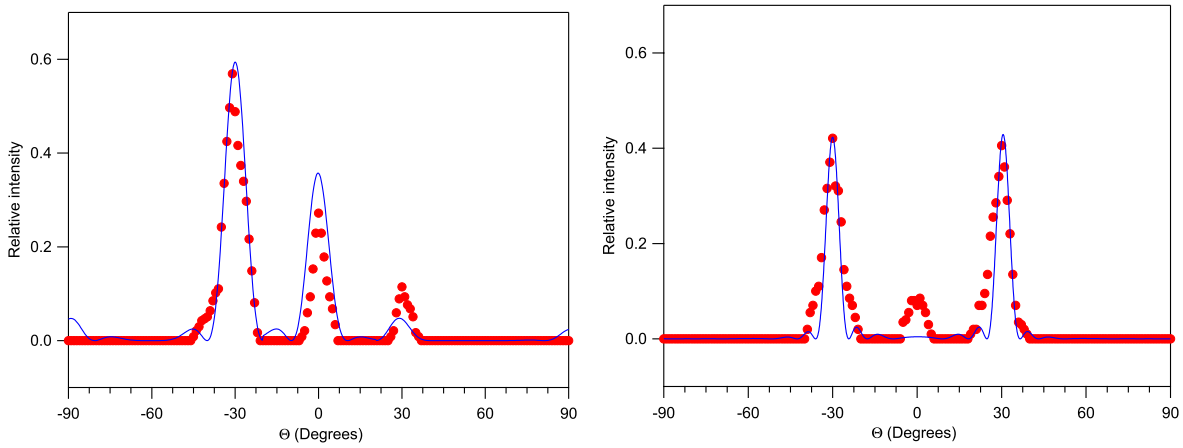

Fig.1 : Results for blazed (left) and regular (right) gratings . Gratings were designed for a first order output at 30 degrees for 0.2THz. Theoretical curves are shown in blue, with red data points

[1] L.H. Lo and R. Leonhardt, *Opt. Express* **16** 20, 15991-15998 (2008).

[2] D.C.O'Shea, T.J. Suleski, A.D. Kathman and D.W. Prather, "Diffractive Optics. Design, Fabrication and Test" *The Society of Photo Optical Instrumentation* Engineering, 2004.

[3] R.A. Lewis, *Terahertz Physics* (Cambridge: Cambridge University Press, 2012).

TP16

Combinatorial synthesis of piezoelectric materials using an inkjet printer

F. Marlton, J. Daniels and O. Standard

School of Materials Science and Engineering, University of New South Wales, NSW 2033, Australia.

Piezoelectrics are used in a wide variety of technology applications and currently their best performing compositions are lead-based. Legislative requirements will impose serious restrictions on the use of these lead-based materials in consumer devices over the coming years and currently no viable lead-free alternative exists. A potential pathway for the discovery of such a unique material is through combinatorial techniques. Combinatorial chemistry is the rapid synthesis and analysis of large numbers of compositions, through many combinations of a relatively small number of starting compounds.

Inkjet printing is currently at the threshold of becoming a standard fabrication tool, with a wide range of materials science applications. It is regarded as one of the most promising techniques for the creation of functional metal oxides on various substrates because it has an automatically controlled printing scheme with precise and flexible droplet volumes and offers rapid mass production.

This review outlines the process and challenges for the synthesis of a ternary phase diagram with a compositional resolution of 1% using ceramic suspensions and inkjet printing technologies. Structural analysis of individual compositions will be carried out with scanning beam diffraction measurements from a synchrotron x-ray or neutron source. This has the potential to lead to the development of novel environmentally-friendly lead-free compositions of piezoelectrics and a state-of-the-art combinatorial synthesis technique for functional materials discovery.

FRIDAY
ABSTRACTS

FM1

Phonon Hall effect in the terbium-gallium-garnet: Skew scattering of phonon

M. Mori[a], A. Spencer-Smith[b], O. P. Sushkov[c] and S. Maekawa[a]

[a] *Advanced Science Research Center, Japan Atomic Energy Agency,Tokai 319-1195, Japan.*

[b] *School of Physics, University of Sydney, Sydney 2006, Australia.*

[c] *School of Physics, University of New South Wales, Sydney 2052, Australia.*

When a magnetic field is applied perpendicular to a heat current in a terbium gallium garnet (TGG), $Tb_3Ga_5O_{12}$, a transverse temperature gradient is induced in the third perpendicular direction [1,2]. This is the "phonon Hall effect (PHE)''. Since the effect takes place at low temperature (~ 5 K) in the insulator, there are no mobile charges such as electrons nor holes to assist the thermal transport. Phonons are not charged and hence cannot be affected by the Lorentz force such as the Hall effect. Spin-orbit interaction for phonons is not obvious unlike the spin Hall effect for electrons. Furthermore, the Neel temperature of the TGG is 0.24 K, whereas the TGG is a paramagnet around 5 K, at which the PHE is observed. Hence, at $T = 5$ K, one cannot expect a considerable contribution from magnons unlike the magnon Hall effect. Therefore, an origin of the PHE is non-trivial and a fundamental question in condensed matter physics.

In this talk, we show that the PHE originates from the resonant skew scattering of phonons by quasi-doublet states at superstoichiometric Tb^{3+} ions [3]. Phonons interact with the crystal field due to electrostatic interaction of lattice with electric multipole moments of the ion. Thus, one can see that the scattering originates from the coupling of lattice strain and the quadrupole moments of Tb^{3+} ions. The phonon Hall angle (S), given by the ratio of off-diagonal and diagonal thermal conductivities divided by the magnitude of the magnetic field, is calculated using Boltzmann transport theory. Obtained magnitude of the effect is in agreement with experiments. We show that S significantly grows with temperature at low temperatures characterized by resonance energy.

[1] C. Strohm, G.L.J.A. Rikken and P. Wyder, *Phys. Rev. Lett.* **95**, 155901 (2005).

[2] A.V. Inyushkin and A.N. Taldenkov, *JETP Lett.* **86**, 379 (2007).

[3] M. Mori, A. Spencer-Smith, O.P. Sushkov and S. Maekawa, arXiv:1407.0802.

FM2

Adsorption of CO_2 and CD_4 in UiO-66: a combination of neutron diffraction and modelling

H. Chevreau[a], W. Liang[b], G.J. Kearley[a], S.G. Duyker[a], D.M. D'Alessandro[b] and V.K. Peterson[a]

[a] *Bragg Institute, Australian Nuclear Science and Technology Organisation, Lucas Heights, NSW, Australia.*

[b] *School of Chemistry, University of Sydney, Sydney, NSW 2006, Australia.*

Over the last twenty years, tremendous progress has been achieved in the field of Metal Organic Frameworks. Among these materials, the zirconium terephthalate UiO-66(Zr) [1] has attracted a growing attention because of its interesting thermal, chemical and water stability and has shown to be a promising material for the separation of CO_2/CH_4 gas mixtures.

In order to get a better understanding of its sorption behavior towards CO_2 and CH_4, a Neutron Powder Diffraction (NPD) investigation of UiO-66 loaded with sequential doses of CO_2 and CD_4 has been carried out on the High Resolution Powder Diffractometer instrument "Echidna" at the OPAL reactor (ANSTO, Sydney).

In total, three adsorption sites for CO_2 and three adsorption sites for CD_4 within the UiO-66(Zr) have been located by neutron powder-diffraction then characterised by a combination of first-principles Density Functional Theory (DFT) calculations and Quantum Atoms In Molecules (QTAIM) theory. An example of the first CO_2 adsorption site is given in figure 1.

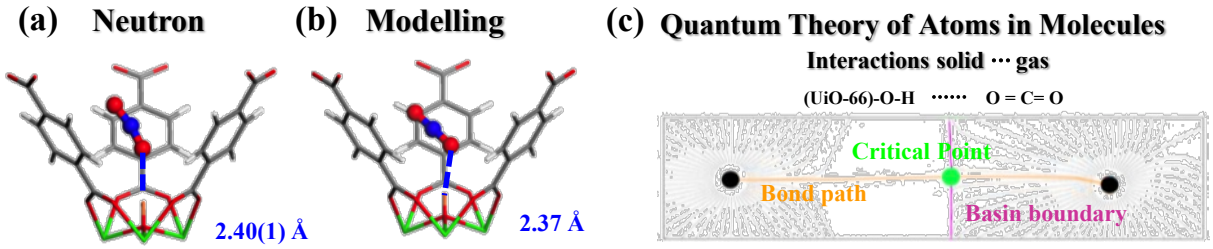

Figure 2. Structure of CO_2 at site Tc_{OH} in UiO-66(Zr) determined using NPD (a) and DFT (b). (c) QTAIM analysis result showing the Gradient field (black lines), bond path (orange line), and basin boundary (where the basin is the region traversed by the paths emanating from the minimum of the density, purple line)

[1] J.H. Cavka, S.R. Jakobsen, U. Olsbye, N. Guillou, C. Lamberti, S. Bordiga and K.P. Lillerud, *J. Am. Chem. Soc.* **130**, 13850 (2008).

FM3

Spin-lattice Coupling and Multiferroic Effects for $3d^4 - 3d^7$ Dopants in a Ferroelectric Host Materials

L. Weston[a], X.Y. Cui[b,c], S.P. Ringer[b,c] and C. Stampfl[a]

[a]*School of Physics, The University of Sydney, Sydney, New South Wales, 2006, Australia.*

[b]*Australian Centre for Microscopy and Microanalysis, The University of Sydney, Sydney, New South Wales, 2006, Australia.*

[c]*School of Aerospace, Mechanical and Mechatronic Engineering, The University of Sydney, Sydney, New South Wales, 2006, Australia.*

The manipulation of spin is of fundamental importance from a device perspective. The electrical control of magnetism is particularly desirable, and the search for materials exhibiting novel magnetoelectric properties currently drives the field of multiferroics [1]. On the microscopic and quantum scale, where one manipulates the spin-state of a single defect or dopant in a semiconductor, lies the field of solitary dopant electronics (solotronics), which represents the fundamental limit of miniaturisation in the study and design of semiconductor spintronic devices [2]. In this work, using first-principles hybrid density functional theory calculations, we have studied spin-lattice coupling effects induced by spin crossover at $3d^4$ – $3d^7$ transition metal dopants in a non-magnetic, ferroelectric $PbTiO_3$ host material. When present at the B-site, a low-spin to high-spin crossover induces marked ferroelectric-like distortions in the local geometry surrounding the dopant, characterised by a shift of the dopant ion with respect to the surrounding O_6 octahedral cage. Analysis of the electronic structure points to a covalent driving force for the distortions, which we explain in terms of the pseudo Jahn-Teller effect (PJTE) [3]. The potential for magnetoelectric coupling arising from the PJTE is also demonstrated; in particular, the possibility for switching the spin-state of the dopant by an electric field is explored.

[1] R. Ramesh and N.A. Spaldin, *Nat. Mater.* **6**, 21 (2007).

[2] P.M. Koenraad and M.E. Flatte, *Nat. Mater.* **10**, 91 (2011).

[3] I.B. Bersuker, *Phys. Rev. Lett.* **108**, 137202 (2012).

Strain-induced magnetic phase transition in $SrCoO_3$ thin films

S.J. Callori[a, b], S. Hu[c], J. Bertinshaw[a, b], Z. Yue[d], S. Danilkin[b], X.L. Wang[d], V. Nagarajan[c], F. Klose[b, e], and J. Seidel[b] and C. Ulrich[a,b]

[a] *School of Physics, The University of New South Wales, Sydney, NSW 2052, Australia*

[b] *The Bragg Institute, Australian Nuclear Science and Technology Organization, Lucas Heights, NSW 2234, Australia.*

[c] *School of Materials Science and Engineering, The University of New South Wales, Sydney, NSW 2052, Australia.*

[d] *Australian Institute for Innovative Materials and Institute for Superconducting and Electronic Materials, University of Wollongong, North Wollongong, NSW 2522, Australia.*

[e] *Department of Physics and Materials Science, City University of Hong Kong, Hong Kong SAR, China.*

Transition metal oxides represent a wide set of materials with a broad range of functionalities, including superconductivity, magnetism, and ferroelectricity, which can be tuned by the careful choice of parameters such as strain, oxygen content, and applied electric or magnetic fields. This tunability makes them ideal candidate materials for use in developing novel information and energy technologies. $SrCoO_3$ provides a particularly interesting system for these investigations. Lee and Rabe have simulated the effect of strain and have predicted that the magnetic state can be tuned through compressive or tensile strain with a ferromagnetic-antiferromagnetic phase transition [1,2]. Such a phase transition would be accompanied by a metal-to-insulator phase transition and a transition to a ferroelectric polarised state.

We have achieved large in-plane tensile strain in $SrCoO_3$ thin films through the proper choice of substrate and our neutron diffraction experiments on only 40 nm thick films have indeed confirmed the transition from a ferromagnetic to an antiferromagnetic ground state, as theoretically predicted [3]. As such, $SrCoO_3$ would constitute a new class of multiferroic material where magnetic and electric polarisations can be driven through external strain.

[1] J.H. Lee and K.M. Rabe, *Phys. Rev. Lett.* **107,** 067601 (2011).

[2] J.H. Lee and K.M. Rabe, *Phys. Rev. B* **84,** 104440 (2011).

[3] S.J. Callori, S. Hu, J. Bertinshaw, Z. Yue, S. Danilkin, X.L. Wang, V. Nagarajan,

[4] F. Klose, J. Seidel and C. Ulrich, submitted to Phys. Rev. B, Rapid. Com. (2014).

FM5

Measuring Liquid Crystal Permittivity With High Accuracy

C. Weickhmann[a], S. Schmidt[a], M. Jost[a], W. Hu[a], R. Jakoby[a],
A. Manabe[b], C. Fritzsch[b] and M. Wittek[b]

[a] *Technische Universität Darmstadt, Institute of Microwave Engineering and Photonics, Merckstr. 25, 64283 Darmstadt, Germany, e-mail: weickhmann@imp.tu-darmstadt.de.*

[b] *Merck KgaA, Darmstadt, Germany.*

Liquid crystals (LC) are a class of anisotropic liquid dielectric materials well-known in the field of display technology since the 1970s. Recently, they have been subject of various investigations from the microwave through the Terahertz range. Their unique property to exhibit local anisotropy allows for tuning using chopped electric fields (DC) and for building various types of tuneable components, e.g. phase shifters. Both loss angle $\tan\delta_{r,LC}$ and permittivity $\varepsilon_{r,LC}$ can be expressed as tensors with respect to the director (i. e. ordinary axis) as

respectively, with typically $\varepsilon_{\parallel} > \varepsilon_{\perp}$ and $\tan\delta_{\perp} > \tan\delta_{\parallel}$. Accurate characterisation of these properties on a macroscopic level is essential for material system optimisation and can reveal information about phase transitions if carried out over a wide frequency range.

In this work, a comprehensive overview of state of the art techniques for characterisation of LCs and liquids in general will be given. The area of application will cover the frequency range from several Gigahertz into the Terahertz range [1]. Non-resonant transmission methods, as largely employed in optics but also in microwave engineering [2], will be considered as well as a resonant technique, namely the cavity perturbation method, which is especially suited for charcterisation of anisotropic material parametres [3]. As an example, ongoing development of a 60 GHz higher-order mode resonant cavity will be presented.

The authors would like to thank Prof. Lewis at Univ. of Wollongong, Merck KgaA and CST AG for their continued support. This work was carried out in the framework of LOEWE STT.

[1] C. Weickhmann, R. Jakoby, E. Constable, and R. Lewis, *IRMMW-THz* (2013).

[2] A. Gaebler, *et al.*, *Microwave Symposium Digest (MTT)* (2010) pp. 1656–1659.

[3] A. Gäbler, F. Gölden, S. Müller, and R. Jakoby, *38th European Microwave Conference, 2008.*, (2008) pp. 909–912.

FM6

Spin Dynamics Simulation of the Magneto-Electric Effect in a Composite Multiferroic Chain

Z. Wang and M. J. Grimson

Department of Physics, University of Auckland, Auckland 1010, New Zealand.

A composite multiferroic chain, i.e. a coupled ferromagnetic-ferroelectric chain, with an interfacial linear magneto-electric coupling is used to study the magnetic and electric responses to external electric or magnetic field [1]. The simulation uses continuous spin dynamics through the Landau-Lifshitz-Gilbert equations of the magnetic spin and the electric pseudo-spin. The dynamics of the electric pseudo-spin are precession free [2]. The simulation provides an accurate description of the distribution of the magnetisation and the polarisation. These studies are based on two groups of microscopic models. One uses the classical Heisenberg model [3] in both of the ferromagnetic and the ferroelectric chains. The other is the classical Heisenberg model in the ferromagnetic chain, but invokes the transverse Ising model [4] in the ferroelectric chain. The results demonstrate that the magnetisation and polarisation are induced by applied electric and magnetic field, respectively. A comparison with the results of related Monte Carlo simulation models is made [5].

[1] A. Sukhov, Chenglong Jia, P.P. Horley and J. Berakdar, *J. Phys.: Condens. Matter.* **22**, 352201 (2010).

[2] Y.M. Jin, Y.U. Wang, A. Kazaryan, Y. Wang, D.E. Laughlin and A.G. Khachaturyan, *J. Appl. Phys.* **92**, 10, p 6172 (2002).

[3] R.W. Gerling and D.P. Landau, *Phys. Rev. B*. **42**, 8214 (1990).

[4] H. Jang and M.J. Grimson, *J. Phys.: Condens. Matter*. **11**, 5045 (1999).

[5] Z. Wang and M.J. Grimson, *AES 2014 Symposium.* In press.

FN1

Commensurate to incommensurate magnetic phase transition in the type-II multiferroic $YBaCuFeO_5$

Y.C. Lai(賴彥仲)[a,b], W.T. Chen(陳威廷)[b], C.W. Wang(王進威)[c], K.C. Rule[d],

F.C. Chou(周方正)[b,c,e] and C.H. Du (杜昭宏)[a]

[a] *Department of Physics, Tamkang University, Tamsui 25137, Taiwan.*

[b] *Center for Condensed Matter Sciences, National Taiwan University 10617, Taiwan.*

[c] *National Synchrotron Radiation Research Center, Hsinchu 30076, Taiwan.*

[d] *Bragg Institute, ANSTO, Kirrawee DC NSW 2234, Australia.*

[e] *Taiwan Consortium of Emergent Crystalline Materials, Ministry of Science and Technology, Taipei 10622, Taiwan.*

The simultaneous existence of magnetic and ferroelectric ordering is a characteristic of multiferroic materials. The search for new multiferroics is partly motivated by the need for non-volatile random access memories for which the electric polarisation (magnetisation) is controlled by magnetic field (electric field) or vice versa. The use of such materials would be extremely beneficial for the next generation of electronic devices (mobile phones, tablets etc) whereby compact size constraints are important as well as optimising reading/writing speeds and power consumption. $YBaCuFeO_5$ has been classified as a type-II multiferroic due to its complex magnetic interactions and low temperature feroelectricity [1]. Two magnetic phase transitions of antiferromagnetic nature have been found near $T_{N1} = 450$ K and $T_{N2} = 170$ K [2]. The first represents the ordering of the Fe^{3+} ions into a commensurate antiferromagnetic state, while the second represents the ordering of the Cu^{2+} ions giving an overall incommensurate antiferromagnetic ground state. For the first time, using modified traveling solvent floating zone growth method, we have been able to grow a centimeter-sized, high-quality, single-crystal of $YBaCuFeO_5$. Magnetisation and neutron diffraction results indicate a complex magnetic phase diagram in this material with a strong hysteresis effect and a chiral magnetic ground state.

[1] D. Khomskii, *Physics* **2**, 20, (2009)

[2] B. Kundys, A. Maignan and Ch. Simon, *Appl. Phys. Lett.*, **94**, 072506, (2009).

Synthesis and Characterisation of ($M_{2-x}Fe_x$)SnO_4 (M = Mn, Zn) Quaternary Transition Metal-Tin-Oxygen Spinel Systems

C. Leung[a], M. Allison[a,b], G. Stewart[c] and T. Söhnel[a]

[a] *School of Chemical Sciences, University of Auckland, Auckland, New Zealand.*

[b] *School of Chemistry, The University of Sydney, Sydney, Australia.*

[c] *School of Physical, Environmental and Mathematical Sciences, UNSW Canberra, Australia.*

Mixed transition-metal oxide (MTMO) spinels including Mn- and Zn-containing stannate phases have promising material properties and are known for their ability to be tailored for particular applications. They are currently being explored as possible alternative substrates in many emerging high-tech applications such as electrode materials in lithium-ion batteries [1] and as conducting oxides in gas detector sensors [2].

This project aims to study the crystal and magnetic structures of the novel iron substituted quaternary stannates ($M_{2-x}Fe_x$)SnO_4 with M = Mn, Zn and $0 \leq x \leq 2$. Neutron and synchrotron X-ray powder diffraction, ^{57}Fe-Mössbauer, IR and UV-Vis spectroscopy, magnetic measurements and SEM/EDX have been performed on these systems to determine the exact mechanism of Fe substitution, the site distribution and oxidation states of the substituted Fe, and its effects on the crystal and magnetic structure.

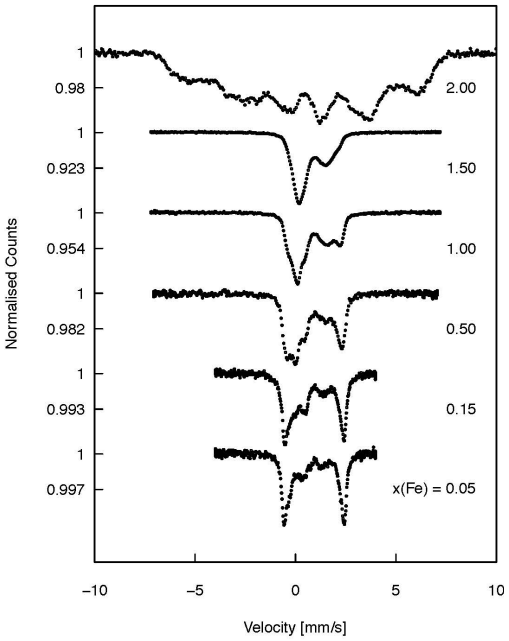

Fig. 1: ^{57}Fe-Mössbauer spectra recorded for ($Zn_{2-x}Fe_x$)SnO_4

Initial results support the hypothesis that the doping mechanism is dependent upon the amount of Fe that is doped. Diffraction results and Mössbauer data indicate that there is an enrichment of Fe relative to Sn for the Fe-rich structures. This might be due to Fe substitution of Zn or Mn for lower concentrations, followed by substitution for Sn as more Fe becomes present in the system.

[1] Y. Xie, X.W. Lou, C. Yuan, H.B. Wu, *Angew. Chem. Int. Ed.* **53**, 1488 (2014).

[2] H.J. Kim, J.H. Lee, *Sensors and Actuators B.* **192**, 607 (2014).

FN3

A combined experimental and computational approach to understanding and developing solid-state ionic conductors

J. Wind and C. Ling

School of Chemistry, University of Sydney, NSW 2006, Australia.

Materials that exhibit significant mobility of different types of charge carriers (oxide ions, protons, electrons) have a range of potential applications including solid-oxide fuel-cell membranes, electrodes, batteries and sensors. A thorough understanding of the fundamental atomic-scale mechanisms of the conduction processes in these materials is necessary to identify ways in which their local chemistry and structure can be modified to lower activation barriers and optimise pathways for conduction.

We have carried out inelastic neutron scattering experiments to probe structural fluctuations that may trigger or facilitate the diffusion process. Together with *ab initio* molecular dynamics (MD) calculations, we are using these results to develop and rigorously verify classical force fields for empirical calculations that will extend the simulations to timescales required to observe actual conduction processes. The results suggest ways in which the local chemistry and structure of materials can be modified to lower activation barriers and optimise the pathways for ionic conduction.

Our initial investigations are focused on apatite-type $Nd_{9.33}Si_6O_{26}$, which is an interesting initial target system for developing this understanding by virtue of its good oxide-ionic conductivity, simple chemical compositions and scope for chemical and structural modification. $Nd_{9.33}Si_6O_{26}$ is a hexagonal apatite structure in space group $P6_3/m$ (two crystallographically distinct Nd sites) with 6.7% Nd vacancies located at the 4f site only. A thorough analysis of different arrangements of Nd vacancy positions has been performed to obtain a suitable input model for *ab initio* MD calculations. Possible arrangements have been classified by the corresponding sum of distances between the vacancies to quantify the degree of distribution and investigate the influence of different vacancy distributions on subsequent calculations.

Magnonic crystals for nanoparticle detection

M. Sushruth[a], R. Begley[a], J. Ding[b], R. Woodward[a], I.S. Maksymov[a], M. Albert[c], W. Wang[c], H. Fangohr[c], A.O.A. Adeyeye[b], M. Kostylev[a] and P.J. Metaxas[a]

[a] *School of Physics, University of Western Australia, Perth, Australia.*

[b] *Electrical and Computer Engineering, National University of Singapore, Singapore.*

[c] *Engineering and the Environment, University of Southampton, Southampton, UK.*

Magnonic crystals (MCs) are nanostructured magnetic metamaterials, which enable geometrical and field-induced control over spin wave propagation and spatially confined ferromagnetic resonances [1]. Here we exploit the magnetic-field dependence of confined ferromagnetic resonance modes in a MC at gigahertz frequencies for magnetic nanoparticle detection. Using field modulated ferromagnetic resonance spectroscopy we show that MNPs captured in an antidot-based MC (Fig. A) modify the MC's resonant eigenmodes. These modifications are manifested as clear resonance field shifts (e.g. Fig. B), which are comparable to the resonance linewidth, a characteristic which is important for sensing. The sign of each mode's resonance field shift predictably depends upon the mode's spatial localisation within the crystal, consistent with the presence of dipole-like fields generated by nanoparticles within the antidots. These shifts are well reproduced via time domain and direct eigenmode-based micromagnetic simulations. This work demonstrates the successful use of high frequency precessional magnetisation dynamics for nanoparticle detection and represents an important first step towards frequency-based, nano-scale magnetic biosensing devices. Such devices are expected to have faster response times than conventional magnetoresistive biosensors while retaining high signal to noise ratios at small device sizes [2].

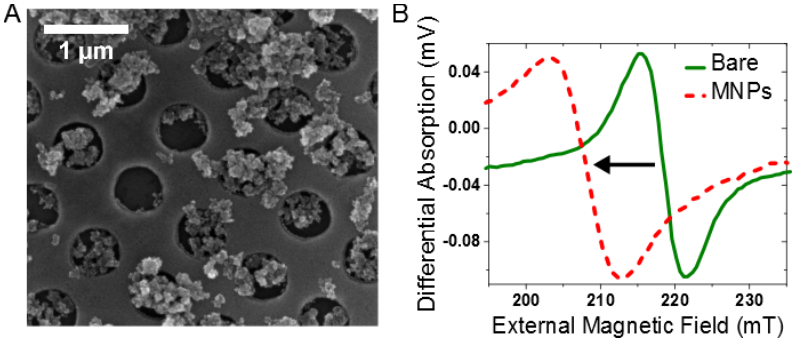

[1] Kruglyak et al., *J. Phys. D: Appl. Phys.* **43**, 264001 (2010).

[2] Braganca et al., *Nanotechnol.* **21**, 235202 (2010).

FN5

Semiconductor Nanowires for Optoelectronics and Energy Applications

C. Jagadish

Research School of Physics and Engineering, The Australian National University, Canberra, ACT0200, Australia.

Semiconductors have played an important role in the development of information and communications technology, solar cells, solid state lighting. Nanowires are considered as building blocks for the next generation electronics and optoelectronics. In this talk, I will introduce the importance of nanowires and their potential applications and discuss about how these nanowires can be synthesized and how the shape, size and composition of the nanowires influence their structural and optical properties. I will present results on axial and radial heterostructures and how one can engineer the optical properties to obtain high performance optoelectronic devices such as lasers, solar cells. Future prospects of the semiconductor nanowires will be discussed.

AUTHOR INDEX

Tuesday 3.02.15	Wednesday 4.02.15		Thursday 5.02.15		Friday 6.02.15	
	7:30 Breakfast		7:30 Breakfast		7:30 Breakfast	
	08:45 **Opening – RA Lewis**		08:45 TM1 A Bruno-Alfonso (Invited)	**Chair: C. Ulrich**	08:45 FM1 M Mori (Invited)	**Chair: O. Sushkov**
	09:00 WM1 F Liu (Invited)	**Chair: C. Zhang**	09:15 TM2 R Skelton		09:15 FM2 H Chevreau	
	09:30 WM2 JSO Evans		09:30 TM3 M Allison		09:30 FM3 L Weston	
	09:45 WM3 M Kostylev		09:45 TM4 PJ Graham		09:45 FM4 C. Ulrich	
	10:00 WM4 T Tahyama (Invited)		10:00 TM5 ML Tate		10:00 FM5 C Weickhmann	
			10:15 TM6 QY Ren		10:15 FM6 ZD Wang	
	10:30 Morning Tea		**10:30 Morning Tea**		**10:30 Morning Tea**	
	11:00 WN1 JC McCallum (Invited)	**Chair: K. Rule**	11:00 TN1 W Koshibae (Invited)	**Chair: M. Kostylev**	11:00 FN1 K Rule	**Chair: G. McIntyre**
	11:30 WN2 S Rogge		11:30 TN2 C Ling		11:15 FN2 T Söhnel	
	11:45 WN3 JP Evans		11:45 TN3 HD Scammell		11:30 FN3 J Wind	
	12:00 ERA M Nicol [ARC] (Invited)		12:00 TN4 GP Cousland		11:45 FN4 M Sushruth	
			12:15 TN5 Y Du		12:00 FN5 C Jagadish (Invited)	
			12:30 Lunch		**12:30 Awards & Closing RA Lewis**	
	12:45 Lunch				**12:45 Lunch**	
	14:00 WA1 IR Evans (Invited)	**Chair: W. Hutchinson**	14:00 TA1 J Seidel (Invited)	**Chair: C. Ling**		
	14:30 WA2 WE Purches		14:30 TA2 C Lueng			
	14:45 WA3 IS Maksymov		14:45 TA3 WT Lee			
	15:00 WA4 C Yin (Invited)		15:00 TA4 NN Elewa			
			15:15 TA5 G McIntyre			
	15:30 2 minute poster clips		15:30 2 minute poster clips			
16:00 Registration	**16:00 Afternoon Tea and Posters WP1-16**		**16:00 Afternoon Tea and Posters TP1-16**			
18:00 Dinner 19:30			**18:00 Dinner**			
	18:30 Conference Dinner After-Dinner Talk Gail Iles (Invited) 22:00		**19:30 Trivia Quiz 22:00**			